13 Egypt. J. Geo. Vol. 67, pp: 219-241 (2023)

Egyptian Journal of Geology

https://egjg.journals.ekb.eg

Source identification, pollution status, and ecological risk assessment of heavy metals contamination in a highly populated unplanned industrial area (Wadi El-Qamar), Alexandria, Egypt

Mouataz T. Mostafa[1*], Habash El-Nady[2], Ramadan M. Gomaa[3], Salman A. Salman[4], and **Ibrahim H. Khalifa[5]**

(1) *Geology Department, Faculty of Science, Arish University, Giza 45511, Egypt*
(2) *Geology Department, Faculty of Science, Arish University, Mansoura 35516, Egypt*
(3) *Geology Department, Faculty of Science, Arish University, North Sinai 45511, Egypt*
(4) *Geological Sciences Department, Inorganic Chemical Industries and Mineral Resources Research Division, National Research Centre, Giza 12622, Egypt*
(5) *Geology Department, Faculty of Science, Suez Canal University, Ismailia 41522, Egypt*

Based on the contents of heavy metals (Co, Cr, Cu, Fe, Mo, Mn, Pb, and Zn) in 22 road dust samples, the urban environmental quality of Wadi El-Qamar area was evaluated. It is a residential area suffering from unplanned industrial activities, overpopulation, and uncontrolled urbanization. Heavy metal sources and geochemical associations were deciphered using a multivariate statistical approach, while the contamination degree and ecological risks were identified using various pollution indices. Moreover, the human health risks (carcinogenic and non-carcinogenic) for residents were estimated via different exposure pathways. The mean abundances of elements were as follows: Fe > Mn > Zn > Cr > Cu > Pb > Mo > Co, while the individual contamination grades decreased in the following order: Mo > Cu > Zn > Pb > Cr > Fe > Mn > Co, according to the geoaccumulation index (I_{geo}) and the contamination factor (CF) average values. The high correlation between Zn and Cu (r = 0.92) reflected their common origin (traffic-related emissions). Notably, only Cu showed individual ecological risk; meanwhile, the overall ecological risk index (RI) classified the study area as having low ecological risk (RI < 150), with an average of 75.20. The health risk assessment indicated the absence of adverse non-carcinogenic risks and the presence of unacceptable carcinogenic risks posed by Cr and Pb. Ultimately, heavy-duty vehicular emissions (e.g., tire and brake wear) and industrial emissions from cement and refining companies are likely the main contributors to heavy metal loadings in the study area. The results of this research will be useful in developing strategies for pollution control and management and can be utilized for comparison in future studies.

Keywords: Industrial emissions, Urban planning, Road dust, Anthropogenic contamination.

1. Introduction

Unplanned urbanization and uncontrolled industrial activities lead to the rapid degradation of urban environmental quality, especially in large cities (Aguilera et al., 2021; Kabir et al., 2021). Being a temporary sink of heavy metal pollutants, road dust (RD) contamination has become a major environmental issue in an urban context (Choi et al., 2020; Gopal et al., 2017). RD particles are composed mainly of quartz and feldspar, in addition to a mixture of solid materials (organic and inorganic) and liquid particles accumulated along pavements (Al-Shidi et al., 2021; Kamani et al., 2018). The chemical composition of RD can be continuously altered as a result of the complex mixing actions that occur during various on-road activities (Bourliva et al., 2017). RD originates from several input sources, which can be categorized into natural and anthropogenic sources. Natural sources are attributed mainly to natural geochemical processes such as soil formation and erosion (Cao et al., 2018), whereas anthropogenic sources include metallurgical activities, burning of

*Corresponding author e-mail: mouataz.t.mostafa@sci.aru.edu.eg; moataz.tarek.m8@gmail.com
Received: 29/07/2023; Accepted: 28/08/2023
DOI: 10.21608/EGJG.2023.225644.1055

fossil fuels, waste incineration, and traffic-related emissions from the exhaust and non-exhaust parts (Jiménez et al., 2018; Sultan et al., 2022; Žibret, 2019). For example, Cr and Zn contents in RD are reported to be derived from braking and tire wear (Hong et al., 2020).

Recently, numerous studies have been carried out to investigate the high concentrations of heavy metals in RD and their ecological and health implications, especially in megacities with high traffic loadings and uncontrolled industrial emitters (Duong & Lee, 2011; Ebqa'ai & Ibrahim, 2017; Logiewa et al., 2020; Yang et al., 2010; Zgłobicki et al., 2019; Zhao et al., 2015). Chronic exposure to toxic metals, such as lead, cadmium, and arsenic, increases the risk of kidney and liver failure, infertility, mental illness, cancer, and nervous breakdown (Khan et al., 2011). The risks associated with these pollutants become more serious as wind, street sweeping, and vehicle-generated turbulence resuspend these particles in the air, causing them to become inhalable (Amato et al., 2014; Žibret, 2019). Correspondingly, metals in RD are susceptible to getting deposited in the circulatory system through ingestion due to their high chemical mobility. Additionally, they can be washed off by road runoff and enter the water bodies, causing highly toxic impacts on the aquatic organisms (Zafra et al., 2017). Noteworthy, RD is regarded as an indicator of urban environmental quality (Li et al., 2016; Najmeddin et al., 2018), as it acts as both a sink and a source of environmental pollutants (Huang et al., 2016). Compared to other urban sediments such as urban soils, roadside plants, and gully sediments, RD has a greater capacity for the adsorption of HMs from the atmosphere (Liu et al., 2019; Shahab et al., 2020). Consequently, it is considered a valuable environmental matrix for monitoring urban pollution.

Wadi El-Qamar area, an industrial and residential district located in the western coastal sector of Alexandria Governorate, is heavily affected by the industrial emissions of the unplanned complex industrial center (cement production, chemical industries, and petrochemicals), in addition to vehicle emissions from cars and heavy-duty vehicles. The proximity of the industrial complex to residential areas, especially with the use of coal as fuel in a number of factories and the emission of cement dust, has increased the potential ecological and health risks (Jadoon et al., 2021). Additionally, several industrial plants near the coast discharge their effluents into the Mediterranean Sea (Okbah et al., 2013; Shreadah et al., 2015). These factors together contribute to worsening the environmental conditions, and therefore, RD is suggested to be loaded with elevated levels of heavy metals in the study area, making it more serious than normal. Concerning the dearth of studies regarding RD pollution in the study area, this study aimed to form a more comprehensive knowledge about RD contamination and the environmental impacts of Wadi El-Qamar complex industrial center as an unplanned industrial area. Accordingly, the study was conducted to (a) ascertain the levels and evaluate the distribution of selected heavy metals in RD, (b) detect critical points with high contamination grade, (c) decipher the geochemical associations among the investigated metals and identify main pollution sources, and (d) estimate the potential health risks to residents and factory workers through different exposure pathways.

2. Materials and Methods

2.1 Site description and road dust sampling

Wadi El-Qamar, the study area is situated between latitudes 31° 8' and 31° 6' N and longitudes 29° 50' and 29° 51' E (Fig. 1a), is an unplanned residential and industrial area located in the west of Alexandria Governorate, the second economic capital of Egypt. Alexandria is a major tourist, industrial, and harbor center located in northern Egypt on the Mediterranean coast, about 216 km from the capital, Cairo. It is inhabited by more than 5 million people and characterized by a desert climate, exhibiting two seasons: the dry, hot season between May and October and the mild, wet season between November and April (Jadoon et al., 2021). The prevailing wind direction is north, which blows across the Mediterranean, resulting in a less severe climate than the desert regions (El-Geziry, 2021). The study area lies in the west of Alexandria, which is considered a growing commercial hub, containing several seaports, such as the Eastern Port and Dekheila Port, and industrial activities, represented, for example, in crude oil refineries and cement factories. What is striking is the presence of residential buildings almost without spatial separation from these industrial facilities, and thereby the residents of this area are directly exposed to emissions from vehicles and factories.

In dry and windless climatic conditions, a systematic sampling of 22 road dust samples (Q1-

Q22) (combining 5 subsamples; 200 g) was conducted using pre-clean polyethylene brushes and plastic dustpans, where the sampling points were homogeneously distributed from both sides along the paved main road of Wadi El-Qamar area, which crosses the industrial area with a length of approximately 8 km and is dominated by heavy-duty vehicles (Fig. 1b). To collect the sample, dust was swept within a 2.5-m radius circle around each sampling site from the impervious surfaces (where the road meets the curb). This sampling protocol, despite its simplicity, continues to be regularly used in investigations of this kind (e.g., Alsanad & Alolayan, 2020; Kabir et al., 2021; Zgłobicki et al., 2019). During sampling, it was taken into consideration to record the coordinates of each sample using a hand-held GPS (Garmin eTrex 30), wear hand gloves and nose masks, avoid sampling near construction sites, conduct sampling in the morning hours (low traffic loads), and sweep the dust gently to minimize the disturbance and resuspension of the fine particles. Samples were packed up in self-sealing polyethylene bags, labeled, and transported to the laboratory, where they were air-dried at room temperature (about 27 °C) for 3 days, homogenized using a ceramic mortar and pestle, and passed through a 63-µm sieve. This fraction was used for analysis, as it is more likely to be resuspended, adheres easily to the hands, contains high metal loadings, and is thereby associated with higher health risks (Charlesworth et al., 2011; Logiewa et al., 2020; Saeedi et al., 2012).

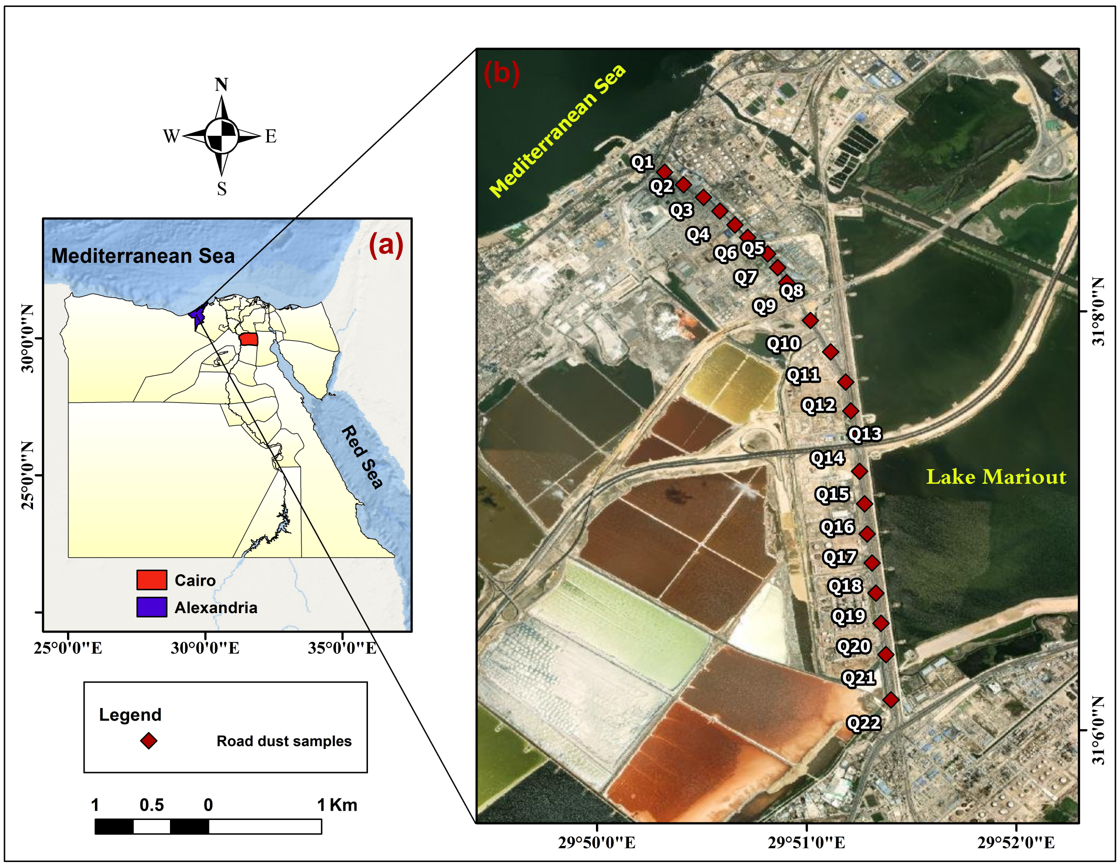

Fig. 1. (a) Location of Wadi El-Qamar area, Alexandria (the study area) and (b) RD sampling points (Q1-Q22).

2.2 Chemical analysis procedures

For elemental total form extraction, the acid digestion procedures suggested by the US Environmental Protection Agency (USEPA) (method 3050B) were followed using a mixture of HNO_3 (70%), HCl (70%), and HF (40%) (9:3:1) (USEPA, 1996a). The digested samples were transferred to a 50 mL volumetric flask, filtered, and diluted with ultra-pure water to the mark. Subsequently, concentrations of Co, Cr, Cu, Fe, Mo, Mn, Pb, and Zn were analyzed using an ICP-AES (inductively coupled plasma atomic emission spectrometry; iCAP-6500 Duo, Thermo Scientific, UK). All the analytical work was conducted at the central laboratory of the Desert Research Center, Egypt. Limits of detection (LOD) were 0.001, 0.01, 0.006, 0.02, 0.002, 0.001, 0.008, and 0.0006 mg/kg for Co, Cr, Cu, Fe, Mn, Mo, Pb, and Zn, respectively.

To provide quality assurance (QA) and quality control (QC), some procedures, including three analytical duplicates and calibrating the instrument using a calibration blank, were applied. Moreover, all the reagents used for analysis were of high analytical grade and superior purity. Additionally, the analytical precision and accuracy were checked by analyzing certified reference materials from the Merck Company (Darmstadt, Germany) and the National Institute of Standards and Technology (NIST), exhibiting ratios of recoveries of 87-113% for all investigated metals.

2.3 Statistical analysis

Descriptive statistics were applied to the data acquired from the geochemical analysis to characterize the contents of HMs, while multivariate statistical techniques, including principal component analysis (PCA), cluster analysis (CA), and Pearson correlation coefficient analysis, were used to decipher the origin of the HMs and elucidate the interrelationships between them. PCA was applied by Varimax normalized rotation to reduce the number of independent variables by generating substitute parameters (the principal components). Each component is composed of a group of metals that are presumed to have a similar origin (Zgłobicki et al., 2018). Furthermore, CA was performed to provide additional information about the mutual relationships of data based on their similarity by determining the geometric, multidimensional Pearson's distances between the investigated elements using Ward's method. Pearson correlation was employed to confirm the results of PCA and CA by defining the strength of a linear relationship between two metals, which reveals information in terms of their origin and geochemical characterizations (Pellinen et al., 2021). All statistical analyses were conducted using IBM SPSS (version 23) and Minitab (version 17) software packages, while, for graph drawing, OriginPro software (2021) was used.

2.4 Pollution assessment methodology

The geo-accumulation index (I_{geo}) is widely applied to distinguish natural and anthropogenic influences on metal enrichment in different environmental matrices (Cai et al., 2021; Malakootian et al., 2021). It was computed through Eq. (1), where C_n represents the measured content of the target HM in RD samples (mg.kg^{-1}), and B_n is the content of this HM in the background. Factor (1.5) is the background matrix correction factor to adjust the natural fluctuations in HM contents and detect very slight anthropogenic influences (Trujillo-González et al., 2016). Notably, due to the difficulty of determining local geochemical reference values for RD being a mobile matrix, the average elemental contents in the upper continental crust, reported by Wedepohl (1995), were used as reference values. According to the precious scale of Muller (1969), I_{geo} values were classified into seven categories (Table 1).

$$\left(I_{geo}\right)_n = \log_2\left(\frac{C_n}{1.5 \times B_n}\right) \quad (1)$$

The contamination factor (CF) is an individual pollution index used to identify pollution levels (Kabir et al., 2021; Shimod et al., 2022). It can be calculated by normalizing the content of the target HM in the RD sample (C_{sample}) by the local background concentrations in the earth crust ($C_{background}$), which were the background values of Wedepohl (1995) in this study (Eq. 2) (Hakanson, 1980; Yesilkanat & Kobya, 2021). Sediment contamination levels based on CF results were briefed in Table 1.

$$CF = \frac{C_{sample}}{C_{background}} \quad (2)$$

The pollution load index (PLI) was applied to determine the overall contamination grade regarding the combined impact of all investigated metals (Tomlinson et al., 1980; Varol, 2011) and calculated through Equation (3), where CF is the contamination factor of each HM and n is the number of analyzed HMs. Notably, PLI values greater than unity are associated with deterioration in sediment quality, denoting that pollution exists, whereas PLI values less than unity reveal that the sediment quality is perfect (no metal pollution) (Hakanson, 1980).

$$PLI = \left(CF_1 \times CF_2 \times CF_3 \times \ldots \times CF_n\right)^{\frac{1}{n}} \quad (3)$$

The enrichment factor (EF) was used to investigate the degree of metal enrichment from natural and anthropogenic sources depending on a reference element (widely used elements are Fe, Al, and Mn) to control the variations caused by heterogeneous samples (Bourliva et al., 2017; Wu et al., 2015; Yuen et al., 2012). It was computed using Equation (4) according to Buat-Menard and Chesselet (1979), where C_x is the measured concentration of the metal x in the sample, C_{ref} is the measured concentration of the chosen reference element in the sample, B_x is the geochemical background value of the target element in the upper continental crust (Wedepohl, 1995), and B_{ref} is the corresponding background concentration of the reference element. In this study, Fe was chosen as a reference element owing to its ability to associate with fine-grained sediments, its uniform natural concentrations and abundance in the Earth's crust, and the similarity of its geochemical characteristics with those of HMs (Bhuiyan et al., 2010; Ekoa Bessa et al., 2022). Values of EF lower than 1.5 were considered to originate mainly from natural processes (e.g., weathering), whereas values higher than 1.5 are assumed to reveal anthropogenic inputs of HMs (e.g., traffic emissions) (Liu et al., 2015; Wang et al., 2008).

$$EF = \frac{\left(\frac{C_x}{C_{ref}}\right)\text{Sample}}{\left(\frac{B_x}{B_{ref}}\right)\text{Background}} \quad (4)$$

Depending on the toxicity limit of each HM, and the biological response to this toxicity level, the individual ecological risk factor (Er) and the overall ecological risk index (RI) were applied to evaluate the potential ecological threats to the biological community posed by single and multiple toxic metals, respectively (Guo et al., 2012; Maanan et al., 2015), computing as specified in Equations (5) and (6). Notably, T_r^i denotes the biological toxic-response factor for a given element, which was estimated and defined for Mn (1), Co (5), Cr (2), Cu (5), Pb (5), and Zn (1), according to Hakanson (1980). Interpretations for these calculations were presented in Table 1.

$$Er = T_r^i \times CF^i \quad (5)$$

$$RI = \sum_{i=1}^{n} Er \quad (6)$$

Table 1. Classification grades of the pollution indices used in this study.

I_{geo} (Muller, 1969)		**CF** (Hakanson, 1980; Yesilkanat & Kobya, 2021)	
≤ 0	Class 0: Uncontaminated	≤ 1	Class 1: Low contamination
0-1	Class 1: Uncontaminated to moderately contaminated		
1-2	Class 2: Moderately contaminated	1-3	Class 2: Moderate contamination
2-3	Class 3: Moderately contaminated to heavily contaminated		
3-4	Class 4: Heavily contaminated	3-6	Class 3: Considerable contamination
4-5	Class 5: Heavily contaminated to extremely contaminated		
> 5	Class 6: Extremely contaminated	> 6	Class 4: Very high contamination
Er (Guo et al., 2010; Hakanson, 1980)		**RI** (Hakanson, 1980; Mostafa et al., 2023).	
< 40	Low risk	<150	Low risk
40-80	Moderate risk	150-300	Moderate risk
80-160	Considerable risk	300-600	Considerable risk
160-320	High risk	≥ 600	High risk
≥ 320	Very high risk		

2.5 Health risk assessment model

This study evaluated the human health risks associated with exposure to cancer-causing and non-cancer-causing HMs in road dust, based on the health risk assessment model that was developed by the USEPA (2002a, 2004), consisting of four key procedures: data measurements, exposure evaluation, dose-reaction evaluation, and health risk estimation (Dat et al., 2021; Rahman et al., 2021; USEPA, 2011). Notably, adults and children are isolated due to the physiological variations between them (Kelepertzis, 2014). The average daily doses (ADD, [mg/(kg/day)]), representing the doses received through ingestion, inhalation, and dermal contact could be estimated using Equations (7)–(9), which were recommended by the USEPA (1989, 1996b, 2011), while the relevant parameters used in these calculations were listed and described in Table 2.

$$ADD_{ingestion} = \frac{C_n \times IR_{ing} \times ED \times EF}{BW \times AT} \times CF \quad (7)$$

$$ADD_{inhalation} = \frac{C_n \times IR_{inh} \times ED \times EF}{BW \times AT \times PEF} \quad (8)$$

$$ADD_{dermal} = \frac{C_n \times SA \times AF \times DAF \times ED \times EF}{BW \times AT} \times CF \quad (9)$$

For evaluation of non-carcinogenic risk, the calculated ADDs (mg/kg/day) for each element of interest and an individual pathway was divided by the corresponding reference dose (RfD) to yield the hazard quotient (HQ, Eq. 10) (USEPA, 2011). According to the Integrated Risk Information System (IRIS), RfD can be defined as an estimation of the maximum appreciable risk level of each metal that does not cause deleterious effects in the human body during a lifetime, as listed in Table 3 (USEPA, 2012). HQs were subsequently summed to compute the total health risk of non-carcinogenic elements through multiple exposure pathways (hazard index, HI). In particular, if HQ and HI values are less than 1.0, no adverse non-carcinogenic risks are believed to occur;

conversely, when these values exceed 1.0, there is a potentiality for non-carcinogenic risks, considering that unity is the threshold reference value (Diami et al., 2016; USEPA, 2002b; Xu et al., 2013).

$$HQ = \frac{ADD}{RfD} \quad (10)$$

HM carcinogenic risks were assessed for each exposure pathway using the individual carcinogenic risk (CR, Eq. 11) and summed to yield the total carcinogenic risk (TCR), depending on the cancer slope factor (CSF), the plausible upper-bound estimate of the biological response to a potential carcinogen, and the calculated average daily dose (ADD) (USEPA, 2002a, 2005). Due to the unknown values of CSF for some HMs, or according to the fact that some metals are not considered to create cancer (e.g., iron), this study evaluated the carcinogenic risks for only four metals (Pb, Cr, Cd, and Ni) (Table 3). For data interpretation, the CR and TCR value of 1×10^{-4} was the acceptable threshold as the exceeding values imply potential lifetime carcinogenic risks (unacceptable high carcinogenic risks).

$$CR = ADD \times CSF \quad (11)$$

Table 2. Description of exposure parameters used for ADD calculations.

Symbol (unit)	Parameter	Value: Children	Value: Adults	Reference
IR_{Ing} (mg/d)	Ingestion rate	200	100	(USEPA, 1996b, 2002b)
ED (yr)	Exposure duration	6	24	(USEPA, 2002b)
EF (d/yr)	Exposure frequency	350		(USEPA, 1996b)
BW (kg)	Average body weight	15	70	(USEPA, 2002b)
AT (d)	Averaging time	365 × ED		(Dat et al., 2021; Malakootian et al., 2021)
IR_{Inh} (m^3/d)	Inhalation rate	7.63	20	(Ferreira-Baptista & De Miguel, 2005; USEPA, 2002b; Xu et al., 2013)
PEF (m^3/kg)	Particle emission factor	1.36×10^9		(USEPA, 1996b, 2002b, 2011)
SA (cm^2)	Exposed skin surface area	2800	5700	(Dat et al., 2021; USEPA, 2002b)
AF (mg/cm^2/d)	Skin-soil adherence factor	0.2	0.07	(USEPA, 2002b)
DAF (unit-less)	Dermal absorption factor	0.001		(USEPA, 2002b)
CF (kg/mg)	Conversion factor	1×10^{-6}		(USEPA, 2002b)

Table 3. Reference doses (RfD) and cancer slope factors (CSF) for toxic HMs via different exposure pathways (Adimalla, 2020; Dat et al., 2021; Malakootian et al., 2021; Tan et al., 2018; USEPA, 2002b, 2011, 2012).

HMs	Reference dose (RfD) (mg/kg/d)			Cancer slope factor (CSF) (mg/kg/day)
	Ingestion	Inhalation	Dermal contact	
Pb	3.50E-03	3.52E-03	5.25E-04	8.50E-03
Co	2.00E-02	5.71E-06	1.60E-02	-
Cr	3.00E-03	2.86E-05	6.00E-05	5.00E-01
Cu	4.00E-02	4.02E-02	1.20E-02	-
Zn	3.00E-01	3.00E-01	6.00E-02	-

3. Results and discussion

3.1 Concentrations and spatial distribution of HMs in road dust

Abundances of Co, Cr, Cu, Fe, Mn, Mo, Pb, and Zn in analyzed urban RD samples fluctuated from 0.72 to 8.74, 29.31 to 121.22, 27.76 to 165.83, 8309 to 22350, 163.48 to 333.32, 7.36 to 46.22, 17.16 to 119.10, and 111.51 to 451.33 mg/kg, respectively. The abundance of elements according to their mean values was as follows: Fe > Mn > Zn > Cr > Cu > Pb > Mo > Co (Table 4). Notably, typical urban elements (Pb, Zn, and Cu) showed skewness and kurtosis values higher than other elements, demonstrating the presence of pollution hotspots (Najmeddin et al., 2018). Moreover, the high coefficient of variation (CV) values of Cu, Pb, Zn, Mo, and Cr associated with relatively high standard deviation (SD) results pointed out that these metals displayed high variability, which can reflect that anthropogenic activities exerted a strong influence on their loadings (Karim et al., 2014). Higher abundance and clear hotspots of HMs were observed in the central zone of the study area, especially Zn, Cr, Cu, Fe, and Mn, where most polluting industrial facilities are situated (mineral oils and refining companies). As contaminants from point sources could be responsible for the localized hotspots (Ekoa Bessa et al., 2022), it seems reasonable to infer that these heavy industrial activities in this zone have led to the release of large amounts of heavy metals. In this regard, Jaradat et al. (2004) reported relatively high Zn levels in street dust samples around a petroleum refinery area in Jordan.

Table 4. The loadings of heavy metals and their descriptive statistics in road dust samples from Wadi El-Qamar area (mg/kg) and average background values.

Sample code	Co	Cr	Cu	Fe	Mn	Mo	Pb	Zn
Q1	2.48	65.27	39.85	10970	225.51	32.17	45.39	138.81
Q2	3.94	77.14	27.76	11080	234.66	26.14	88.78	136.45
Q3	2.42	49.33	28.30	10830	213.14	22.82	32.81	139.73
Q4	2.62	58.77	32.45	10800	242.62	14.55	22.02	141.42
Q5	4.75	48.22	47.41	10890	246.87	11.43	24.04	137.37
Q6	2.21	29.31	49.11	10690	240.29	10.63	34.16	144.62
Q7	5.49	121.22	84.51	19350	325.74	15.19	19.32	239.72
Q8	2.14	100.51	89.25	19604	333.32	7.36	36.85	246.86
Q9	3.14	63.79	73.68	18560	310.54	11.43	51.01	249.12
Q10	0.72	117.85	102.13	21720	313.37	21.41	44.27	205.34
Q11	3.07	74.91	90.59	22350	304.82	23.27	67.87	204.76
Q12	4.58	116.11	109.73	21420	324.41	37.63	50.34	207.16
Q13	0.83	99.31	164.9	19110	314.58	36.24	30.33	451.33
Q14	7.08	87.04	158.56	21080	305.50	46.22	32.81	390.32
Q15	1.25	66.01	165.83	17580	311.34	25.06	28.14	428.81
Q16	1.74	53.77	34.25	12129	189.33	32.31	17.16	162.84
Q17	3.73	51.55	32.86	17140	178.49	15.64	119.10	157.75
Q18	5.66	39.32	27.9	16730	193.71	19.43	60.46	168.77
Q19	3.84	69.71	49.42	17900	228.94	24.44	35.73	221.13
Q20	8.74	78.25	53.19	19890	181.25	22.74	36.54	222.85
Q21	5.96	62.68	50.05	8309	163.48	39.58	26.32	111.51
Q22	4.82	56.52	39.85	9418	173.52	32.26	19.44	112.26
Univariate statistical analysis								
Mean	3.69	72.12	70.53	15798	252.52	24.00	41.95	209.95
Median	3.44	65.64	49.74	17360	241.46	23.05	34.95	186.77
Maximum	8.74	121.22	165.83	22350	333.32	46.22	119.10	451.33
Minimum	0.72	29.31	27.76	8309	163.48	7.36	17.16	111.51
SD	2.06	25.54	45.19	4710	58.80	10.51	24.47	97.18
CV	55.71	35.42	64.08	29.81	23.28	43.81	58.33	46.29
Skewness	0.67	0.58	1.14	-0.19	-0.02	0.34	1.88	1.50
Kurtosis	0.24	-0.40	0.23	-1.65	-1.60	-0.62	3.97	1.57
Geochemical reference values								
[a] Turekian and Wedepohl (1961)	19	90	45	47,200	850	2.6	20	95
[b] Wedepohl (1995)	11.6	35	14.3	30,890	527	1.4	17	52
[c] Kabata-Pendias and Pendias (2001)	6.9	42	14	47,000	418	1.8	25	62

(a) Distribution of the elements in Earth's Crust in sedimentary rocks (shales); (b) Chemical composition of the Continental Crust (Upper Continental Crust); (c) Average HM concentrations for world soils.

SD standard deviation, *CV* coefficient of variation

Mo, Pb, Cu, and Zn exhibited higher average concentrations compared with their corresponding values in the geochemical backgrounds of Turekian and Wedepohl (1961), Wedepohl (1995), and Kabata-Pendias and Pendias (2001) in Earth's Crust sedimentary rocks (shales), Upper Continental Crust, and world soils, figuring out their anthropogenic enrichment in road-deposited sediments (Table 4). Molybdenum contents in the studied RD samples were compared to those of other explorations performed in other countries and revealed that its abundance in this investigation was much higher than those found in other studies (Chatterjee & Banerjee, 1999; Ferreira-Baptista & De Miguel, 2005; Najmeddin et al., 2018; Wang et al., 2020) (Table 5). Moreover, the mean content of Cu was higher in Wadi El-Qamar than in Dhaka, Bangladesh (Safiur Rahman et al., 2019), Greater Calcutta, India (Chatterjee & Banerjee, 1999), Luanda, Angola (Ferreira-Baptista & De Miguel, 2005), Toronto, Canada (Nazzal et al., 2013), and Al-Qunfudah, Saudi Arabia (Harb et al., 2015), and lower than that in Alexandria, Egypt (Jadoon et al., 2021), Nanjing, China (Wang et al., 2020), Ahvaz, Iran (Najmeddin et al., 2018), Lublin, Poland (Zgłobicki et al., 2018), Madrid, Spain (Miguel et al., 1997), Mexico City, Mexico (Aguilera et al., 2021), and Ho Chi Minh, Vietnam (Dat et al., 2021). Based on these comparisons, the Mo contents can generally be classified as exhibiting high accumulation levels, while the Cu, Pb, and Zn concentrations can be classified as showing moderate accumulation levels. Notably, many studies reposted the association of Mo with industrial and traffic emissions (Amato et al., 2014; Vanegas et al., 2021; Wiseman et al., 2021). Consequently, the high values of Mo compared to other cities and geochemical references are explained since both of the mentioned input sources exist in Wadi El-Qamar area.

Table 5. A comparison of toxic metal mean concentrations (mg/kg) in road dust from different cities around the world.

City and country	Co	Cr	Cu	Mo	Pb	Zn	Reference
Wadi El-Qamar, Egypt	4	72	71	24	42	210	This study
Alexandria, Egypt	3	24	80	-	70	169	(Jadoon et al., 2021)
Nanjing, China	11	-	133	4.5	102	281	(Wang et al., 2020)
Dhaka, Bangladesh	-	144	50	-	19	239	(Safiur Rahman et al., 2019)
Greater Calcutta, India	16	54	44	1	536	159	(Chatterjee & Banerjee, 1999)
Ahvaz, Iran	10	52	74	3	85	309	(Najmeddin et al., 2018)
Luanda, Angola	3	26	42	2	351	317	(Ferreira-Baptista & De Miguel, 2005)
Lublin, Poland	-	86	82	-	44	241	(Zgłobicki et al., 2018)
Madrid, Spain	3	61	188	-	1927	476	(Miguel et al., 1997)
Mexico City, Mexico	7	51	100	-	128	281	(Aguilera et al., 2021)
Toronto, Canada	-	198	162	-	183	233	(Nazzal et al., 2013)
Al-Qunfudah, Saudi Arabia	5	-	40	-	26	47	(Harb et al., 2015)
Ho Chi Minh, Vietnam	8	102	154	-	50	466	(Dat et al., 2021)

3.2 Source identification and association of HMs in road dust

The statistical analyses were applied widely to discriminate the sources of HMs (e.g., (Mostafa et al., 2023; Said et al., 2021). The correlation between Zn and Cu was the strongest (r = 0.915), reflecting their mutual dependencies and common origin (traffic emissions) (Table 6). Additionally, the correlation matrix showed strong positive correlations (r > 0.6) among Fe with Cr (r = 0.664), Cu (r = 0.641), Mn (r = 0.668), and Zn (0.623), and Mn with Cu (r = 0.757) and Cr (r = 0.688), pointing out that the mentioned HMs share similar geochemical characteristics and could be bound to Fe and Mn oxides/hydroxides, considering that these marker elements (Fe and Mn) can help in metal source identification (Zhong et al., 2016). According to Dall'Osto et al. (2010), the presence of brake wear in the road dust can be inferred depending on the Fe-Cu correlation, as Cu is used in vehicle brakes to adjust heat transfer (Adachi & Tainosho, 2004; Bourliva et al., 2017), while the wear of brake pads (especially brake rotors and drums) can contribute to Fe accumulation in road dust (Apeagyei et al., 2011). Otherwise, the absence of correlation among Co, Pb, Mo, and other HMs indicated their different geochemical characteristics.

Table 6. Pearson correlation matrix between HM concentrations in road dust samples from Wadi El-Qamar area (*n* = 22 samples).

HMs	Co	Cr	Cu	Fe	Mn	Mo	Pb	Zn
Co	1							
Cr	-0.008	1						
Cu	-0.174	0.582**	1					
Fe	0.054	0.664**	0.641**	1				
Mn	-0.341	0.688**	0.757**	0.668**	1			
Mo	0.212	0.213	0.348	0.001	-0.109	1		
Pb	0.014	-0.073	-0.199	0.214	-0.105	-0.149	1	
Zn	-0.151	0.436*	0.915**	0.623**	-0.638**	0.255	-0.161	1

** Correlation is significant at the 0.01 level (2-tailed).

* Correlation is significant at the 0.05 level (2-tailed).

Three principal components (PCs) with eigenvalues higher than 1 were extracted and allocated for 78.90% of the total variation within the variables (Fig. 2, Table 7). PC1 was mainly loaded with Fe, Mn, Cr, Cu, and Zn, implying that these metals represent contributions from both natural (Fe, Mn) and anthropogenic sources (Cu, Zn, and Cr), which highlights the role of iron and manganese oxides in adsorbing the traffic metals (Cu and Zn). Noteworthy, multiple research projects have recognized that Cu and Zn are associated with traffic emissions (e.g., Budai & Clement, 2018; Choi et al., 2020; Grigoratos & Martini, 2015). Additionally, PC2, which was loaded mainly with Co and Mo, appeared to be a multi-source-related component, and their accumulation can be referred to both natural processes (e.g., soil and asphalt weathering and atmospheric deposition) and anthropogenic inputs to a lesser extent (e.g., metallic vehicle components) for Co (Han et al., 2016; Wiseman et al., 2021) and fly ash and fossil-fuel combustion for Mo (Smedley & Kinniburgh, 2017). For the third PC, it was only highly loaded with Pb, demonstrating its anthropogenic origin (e.g., combustion of fossil fuels, tire wear, lubricant oils for engines, and industrial raw materials) (Bourliva et al., 2017; Guney et al., 2010; Kabir et al., 2021), considering its relatively high concentrations. The individual loading of Pb in this component suggests it has different geochemical characteristics (e.g., immobility and a strongly hydrophobic nature) (Ameh et al., 2016; Liu et al., 2019).

Table 7. Rotated component matrix of HMs in RD samples from Wadi El-Qamar area.

Heavy metals	Principal components		
	PC1	PC2	PC3
Co	-0.13	**0.83**	0.22
Cr	**0.79**	0.12	0.06
Cu	**0.91**	0.02	-0.31
Fe	**0.86**	0.07	0.37
Mn	**0.86**	-0.37	-0.02
Mo	0.20	**0.70**	-0.45
Pb	-0.02	0.03	**0.86**
Zn	**0.84**	0.00	-0.27
Rotation sums of squared loadings			
Eigenvalues	3.69	1.33	1.29
Proportion of variance %	46.10	16.66	16.14
Cumulative % of variance	46.10	62.76	78.90

Rotation Method: Varimax with Kaiser Normalization; Bold values indicate significant loading factors (>0.7)

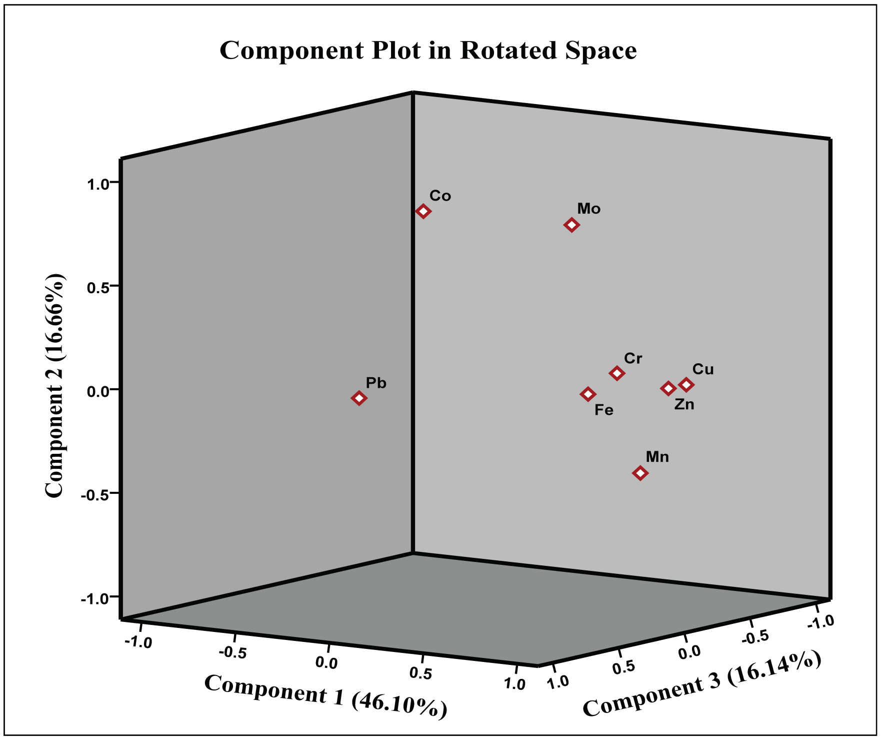

Fig. 2. 3D plot of the principal component analysis (PCA) loadings of HMs in RD samples of Wadi El-Qamar area, Egypt.

Figure 3 shows the results of the cluster analysis (CA) as a dendrogram with five specific clusters. Cluster 1, cluster 2, and cluster 3 were mainly responsible for Co, Mo, and Pb, respectively, suggesting different geochemical characteristics or origins, which are consistent with the correlation analysis results. Moreover, the fourth cluster was dominated by Cr, Mn, and Fe, which confirmed the dominance of the geogenic sources in their enrichment. Several studies have documented the natural origin of Mn in road-deposited sediments (e.g., Al-Khashman, 2007; Fan et al., 2022; Pan et al., 2017). Furthermore, cluster 5 contained Cu and Zn (the traffic marker elements), exhibiting similar geochemical behavior as chalcophile elements.

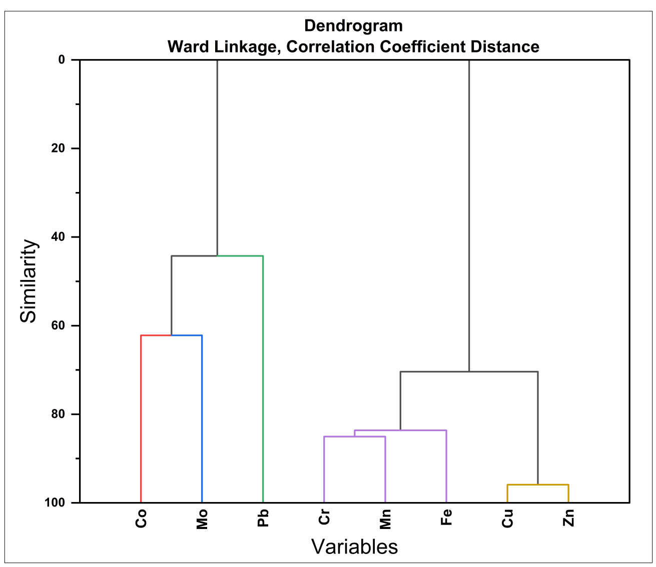

Fig. 3. Cluster analysis (CA) of HMs in RD samples from Wadi El-Qamar area, Egypt.

3.3 Pollution and ecological risk assessment of HMs in road dust

The study found that Igeo values of HMs in the RD samples decreased in the following order: Mo > Cu > Zn > Pb > Cr > Fe > Mn > Co, considering that the highest Igeo value was observed for Mo at the locality of Q14 (Igeo = 4.46, heavily to extremely contaminated) (Fig, 4). This high contamination grade for Mo can be referred significantly to brake pad abrasion (Vanegas et al., 2021; Wiseman et al., 2021), as in general, the brake discs are made up of Fe (about 95%), silica (about 2%), and Mo (about 0.2%) (Hulskotte et al., 2014), regarding the great contribution made by braking-related emissions in the total traffic emissions, with ratios up to 50, 12, and 70% in PM10, PM2.5, and total braking-related emissions, respectively (Bozlaker et al., 2014; Harrison et al., 2012; Hulskotte et al., 2014). Being a geochemical signature for contamination from traffic sources, the comparatively higher Igeo values observed for Cu, Zn, and Pb were mainly attributed to traffic-related emissions (e.g., the deposition of exhaust particles from vehicles) followed by industrial emissions (Aguilera et al., 2021; Choi et al., 2020; Shahab et al., 2020). Otherwise, negative Igeo values were recorded for Co, Fe, and Mn in all sampling sites, which showed that the RD is uncontaminated with these metals, which were minimally affected by anthropogenic influences.

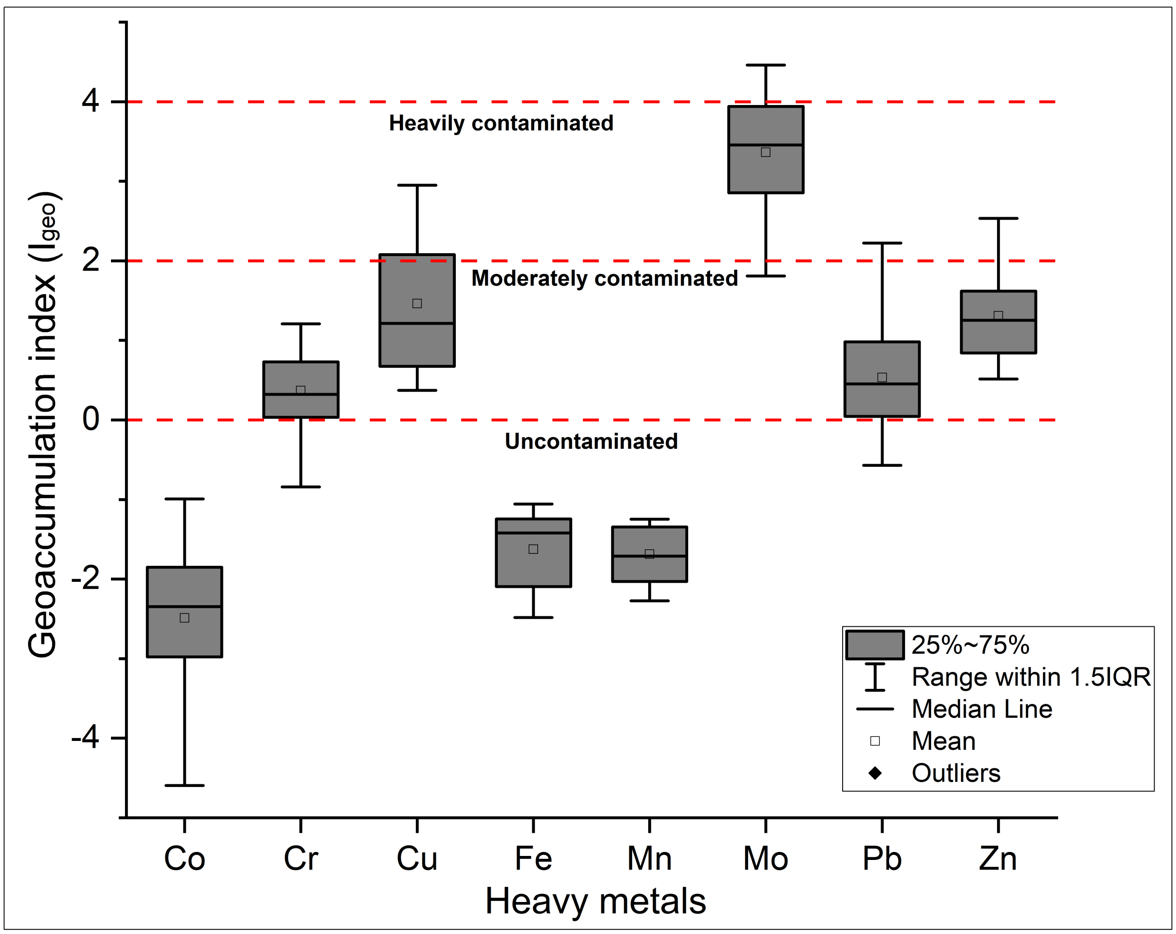

Fig. 4. Box plot of the geoaccumulation index (I_{geo}) for studied HMs in RD samples from Wadi El-Qamar area, Egypt.

Table 8 presents the results of the contamination factor (CF) of eight HMs, which showed that CF values of Mo for nearly all samples were higher than 5.26, demonstrating extremely contaminated road-deposited sediments (CF > 6). By comparison, the hot pollution sites were Q14 for Mo, Q15 for Cu, Q13 for Zn, and Q17 for Pb, falling under class 4 (very high contamination level). The CF values for Cr ranged from 0.84 to 3.46, with an average of 2.06, indicating a moderate contamination level (class 2, 1 < CF < 3). Noteworthy, Cr accumulation in urban RD may be owing to cement kilns, oil refineries, car corrosion, the combustion of fossil fuels, and tire and brake wear (Adamiec et al., 2016; Ekoa Bessa et al., 2021; Mandal & Voutchkov, 2011). In the study area, heavy metal contents (especially Pb, Zn, and Cr) in samples north of the study area are suggested to be related to the atmospheric deposition from the chimney of the Portland Cement plant, as cement production requires a substantial energy supply, which is provided by fossil fuel combustion. In the same context, Cr could also be released due to the friction of the lining for the rotary cement kilns (Banat et al., 2005). This explanation matches what was documented by Mandal and Voutchkov (2011) that the accumulation of Cr, Pb, and Zn in the topsoil around a cement factory in Kingston, Jamaica, was attributed to the shared contribution by the air emissions from cement kilns and vehicles. Furthermore, in agreement with the I_{geo} evaluation, the average CFs of Mn, Fe, and Co were < 1, inferring that these metals exhibited low contamination levels. Regarding an aggregative explanation of the overall pollution degree, PLI values, regardless of the sampling point, were higher than unity, which confirmed that RD sediment quality deteriorated (Table 8). In fact, heavy-duty vehicles generate high friction with the road surface and inevitably contribute more to road wear and traffic emissions when compared to light-duty vehicles (Abu-Allaban et al., 2003; Denby et al., 2013), as the mass of deposited particles from one heavy-duty vehicle can be approximately equal to the mass deposited by fifty light-duty vehicles (Hong et al., 2020). Hence, heavy-duty vehicle volume in Wadi El-Qamar area should be controlled by allowing them to pass during particular periods of the day or setting vehicle weight restrictions.

HM enrichment factors (EFs) for RD samples are shown via violin plot in Fig. 5, which reveals that all studied metals, except for Mn and Co, had EF values higher than the limit value of 1.5, attributed to anthropogenic input sources. Moreover, HMs were ranked according to the enrichment degree as: Mo > Cu > Zn > Pb > Cr > Mn > Co. The EF values for Zn ranged between 5.44 and 14.49, implying a significant enrichment degree (5 < EF < 20), while the EF values for Cr hovered around 4, referring to a moderate enrichment degree.

Table 8. Contamination factor (CF) and pollution load index (PLI) values for heavy metals in road dust samples from Wadi El-Qamar area.

Sites	CF								PLI
	Co	Cr	Cu	Fe	Mn	Mo	Pb	Zn	
Q1	0.21	1.86	2.79	0.36	0.43	22.98	2.67	2.67	1.51
Q2	0.34	2.20	1.94	0.36	0.45	18.67	5.22	2.62	1.67
Q3	0.21	1.41	1.98	0.35	0.40	16.30	1.93	2.69	1.27
Q4	0.23	1.68	2.27	0.35	0.46	10.39	1.30	2.72	1.23
Q5	0.41	1.38	3.32	0.35	0.47	8.16	1.41	2.64	1.32
Q6	0.19	0.84	3.43	0.35	0.46	7.59	2.01	2.78	1.18
Q7	0.47	3.46	5.91	0.63	0.62	10.85	1.14	4.61	1.95
Q8	0.18	2.87	6.24	0.63	0.63	5.26	2.17	4.75	1.71
Q9	0.27	1.82	5.15	0.60	0.59	8.16	3.00	4.79	1.79
Q10	0.06	3.37	7.14	0.70	0.59	15.29	2.60	3.95	1.77
Q11	0.26	2.14	6.33	0.72	0.58	16.62	3.99	3.94	2.11
Q12	0.39	3.32	7.67	0.69	0.62	26.88	2.96	3.98	2.46
Q13	0.07	2.84	11.53	0.62	0.60	25.89	1.78	8.68	2.08
Q14	0.61	2.49	11.09	0.68	0.58	33.01	1.93	7.51	2.74
Q15	0.11	1.89	11.60	0.57	0.59	17.90	1.66	8.25	1.93
Q16	0.15	1.54	2.40	0.39	0.36	23.08	1.01	3.13	1.24

Q17	0.32	1.47	2.30	0.55	0.34	11.17	7.01	3.03	1.62
Q18	0.49	1.12	1.95	0.54	0.37	13.88	3.56	3.25	1.55
Q19	0.33	1.99	3.46	0.58	0.43	17.46	2.10	4.25	1.75
Q20	0.75	2.24	3.72	0.64	0.34	16.24	2.15	4.29	1.95
Q21	0.51	1.79	3.50	0.27	0.31	28.27	1.55	2.14	1.50
Q22	0.42	1.61	2.79	0.30	0.33	23.04	1.14	2.16	1.34
Mean	0.32	2.06	4.93	0.51	0.48	17.14	2.47	4.04	1.71
Maximum	0.75	3.46	11.60	0.72	0.63	33.01	7.01	8.68	2.74
Minimum	0.06	0.84	1.94	0.27	0.31	5.26	1.01	2.14	1.18
Standard deviation (SD)	0.18	0.73	3.16	0.15	0.11	7.51	1.44	1.87	0.40

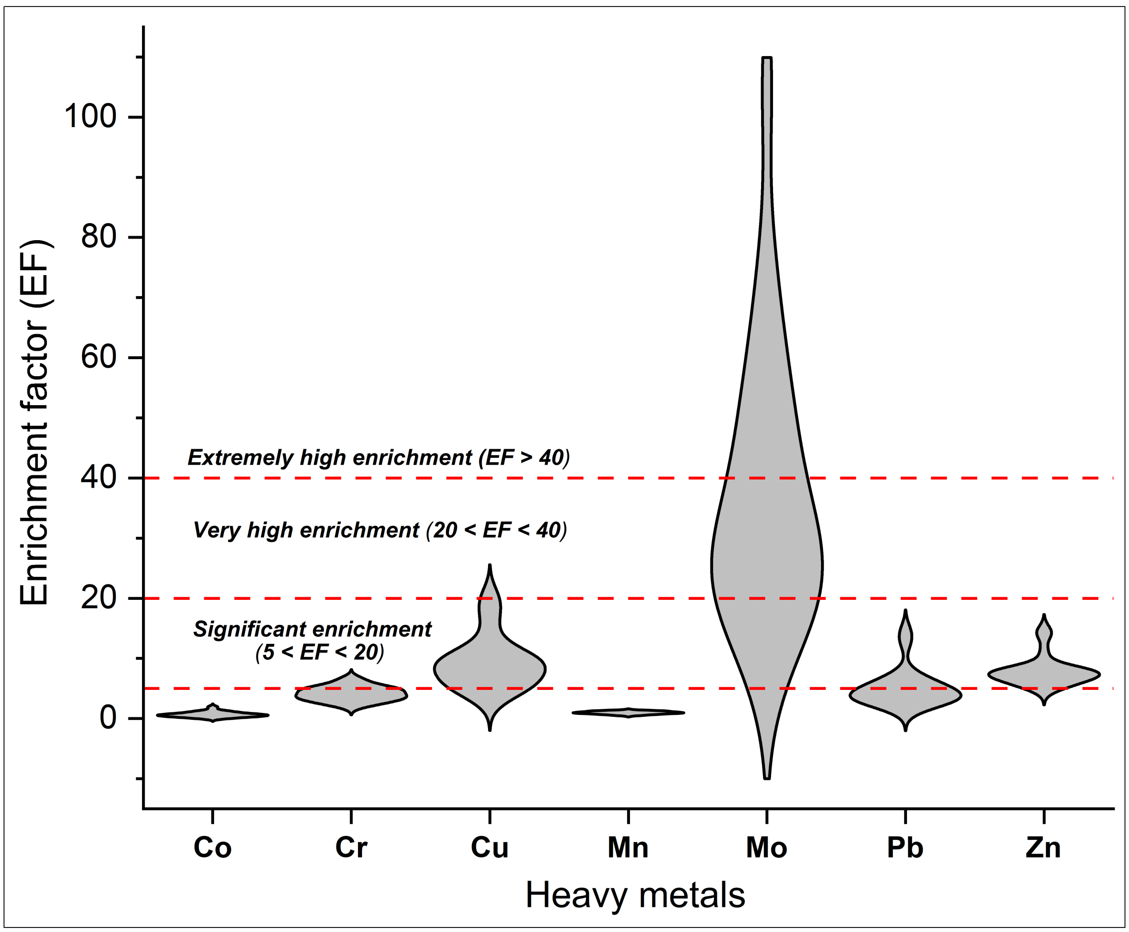

Fig. 5. Violin plot of enrichment factor (EF) for investigated toxic HMs in RD samples, Wadi El-Qamar area, Egypt.

In this regard, anthropogenic sources of Zn in RD particles are primarily from the tear and wear of vehicle tires (as a vulcanization accelerator), diesel exhaust emissions, lubricating oils, and metallurgical industries (Arslan, 2001; Baensch-Baltruschat et al., 2020; Fan et al., 2021; Trojanowska & Świetlik, 2019; Zheng et al., 2010). According to the estimation conducted by Hwang et al. (2016), about 0.57 million kg of Zn were released into the urban environment of South Korea in 2014 due to the mechanical abrasion of vehicle tires. Consequently, to control dust metal enrichment and minimize its loading budget, frequent water washing of street surfaces is suggested, as it is efficient in increasing the mass and surface tension forces for the deposited urban sediments, which subsequently reduces their mobility and mitigates dust resuspension (Amato et al., 2010; Gulia et al., 2019). Moreover, combining dust palliatives during street cleaning activities is an effective mitigating measure for binding fine dust particles together to prevent them from becoming airborne (Polukarova et al., 2020; Tong et al., 2021). Many kinds of chemical dust suppressants are used, such as petroleum-based binders (e.g., cutback asphalt), electrochemical stabilizers (e.g., sulfonated petroleum), and organic non-petroleum chemicals (e.g., lignosulfonates), with no preference for petroleum-based binders due to the possibility of contaminating waterways via urban runoff (Amato et al., 2010).

According to the given interpretation criteria for the individual ecological risk factor (Er), all HMs presented low ecological risks (Er < 40). The exception was copper, which showed a moderate ecological risk in three sites (Q13, Q14, and Q15) (Table 9). In biological systems, Cu is redox-active, having the capability of generating reactive oxygen species like other transition elements, which gives it an ecologically particular concern (Gao et al., 2020; Kelly & Fussell, 2012). In particular, the overall ecological risk index (RI) classified the RD in the study area as having low ecological risk (RI < 150), with an average of 75.20 (Table 9). Notwithstanding, the secondary ecological impacts can occur as a result of entering HMs into the aquatic system of the Mediterranean Sea (as particulate and dissolved phases) through road runoff (Ahmed & Ishiga, 2006; Pang et al., 2015). For instance, Smedley et al. (2014) attributed the elevation of Mo contents in the British surface water to urban and industrial pollution. Therefore, it is also important to sample and geochemically monitor urban runoff after precipitation events, specifically with the unstable climate and wet winter in the study area.

Table 9. Ecological risk results: individual ecological risk factor (Er) and overall ecological risk index (RI) for HMs in road dust samples from Wadi El-Qamar area.

Sites	Er						RI
	Co	Cr	Cu	Mn	Pb	Zn	
Q1	1.05	3.72	13.95	0.43	13.35	2.67	59.59
Q2	1.70	4.40	9.70	0.45	26.10	2.62	71.40
Q3	1.05	2.82	9.90	0.40	9.65	2.69	48.92
Q4	1.15	3.36	11.35	0.46	6.50	2.72	47.97
Q5	2.05	2.76	16.60	0.47	7.05	2.64	54.79
Q6	0.95	1.68	17.15	0.46	10.05	2.78	56.59
Q7	2.35	6.92	29.55	0.62	5.70	4.61	79.49
Q8	0.90	5.74	31.20	0.63	10.85	4.75	84.73
Q9	1.35	3.64	25.75	0.59	15.00	4.79	80.47
Q10	0.30	6.74	35.70	0.59	13.00	3.95	91.93
Q11	1.30	4.28	31.65	0.58	19.95	3.94	92.68
Q12	1.95	6.64	38.35	0.62	14.80	3.98	98.89
Q13	0.35	5.68	57.65	0.60	8.90	8.68	121.29
Q14	3.05	4.98	55.45	0.58	9.65	7.51	118.82
Q15	0.55	3.78	58.00	0.59	8.30	8.25	117.46
Q16	0.75	3.08	12.00	0.36	5.05	3.13	46.81
Q17	1.60	2.94	11.50	0.34	35.05	3.03	82.61
Q18	2.45	2.24	9.75	0.37	17.80	3.25	60.11
Q19	1.65	3.98	17.30	0.43	10.50	4.25	64.34
Q20	3.75	4.48	18.60	0.34	10.75	4.29	68.95
Q21	2.55	3.58	17.50	0.31	7.75	2.14	57.12
Q22	2.10	3.22	13.95	0.33	5.70	2.16	49.49
Mean	1.59	4.12	24.66	0.48	12.34	4.04	75.20
Maximum	3.75	6.92	58.00	0.63	35.05	8.68	121.29
Minimum	0.30	1.68	9.70	0.31	5.05	2.14	46.81
Standard deviation (SD)	0.88	1.46	15.80	0.11	7.20	1.87	23.69

3.4 Human health risk evaluation

Expressed as average daily doses (ADDs), exposure assessment for HMs via dermal, ingestion, and inhalation pathways was employed, as presented in Table 10. Zn and Cr showed the highest exposure doses through the ingestion pathway, which was the most critical exposure pathway. Notably, children are more susceptible to being exposed to HMs as they can easily ingest the contaminated dust by swallowing RD particles during their outdoor play activities, in addition to their lower body weight and higher gastrointestinal absorption rates (Bourliva et al., 2017; Zhang et al., 2017). Several studies have also shown that children have a higher risk compared to adults in contaminated areas (e.g., Cao et al., 2015; Huang et al., 2020); thus, their teachers and parents should make them aware of the need to avoid direct ingestion of RD and to wash their hands before eating. Since the residential areas in the study area are located directly nearby to the factories and on the main road, reducing outdoor activities is recommended to control RD inhalation exposure for local inhabitants, as RD particles exist in the ground-level atmosphere (the living zone). As for people whose nature of work requires them to exist in the streets for long periods (e.g., traffic men and street vendors), they should wear suitable masks, owing to the obvious source-pathway-receptor linkage associated with the direct and chronic exposure to HMs. Jadoon et al. (2021) studied house dust contamination in Alexandria City through pollution indices and revealed a moderate contamination grade of Cu and a high contamination level of Pb, which emphasizes the ability of transfer and the high potential for exposure of the population, even inside their homes through the atmospheric deposition after the resuspension of dust particles.

Generally, HQ and HI values for all studied metals were lower than the safe level of 1, indicating the absence of adverse non-carcinogenic risks posed to the local inhabitants from dust exposure in Wadi El-Qamar area, as shown in Table 10. Particularly, Cr and Pb posed the highest cumulative non-carcinogenic risks for both children (HI = 0.35 and 0.16, respectively) and adults (HI = 0.04 and 0.02, respectively). Compared with adults, children showed higher non-carcinogenic risks, with an average HI value for all studied metals of about nine times that of adults, which confirms the high vulnerability of the children. In regards to the carcinogenic risks through ingestion, the individual carcinogenic risk (CR) values for Cr exceeded the acceptable limit for children and adults (CR = 1×10^{-4}), demonstrating unacceptable carcinogenic risks; meanwhile, Pb posed carcinogenic risks only for children (Table 10). Regarding the inhalation pathway, CR values for Cr were between 1×10^{-6} and 1×10^{-4}, which were considered acceptable and tolerable (moderate carcinogenic risks), whereas CR values for Pb were less than 1×10^{-6}, demonstrating negligible carcinogenic risks. Likewise, the total carcinogenic risk (TCR) related to the three routes of exposure showed high carcinogenic risks of Cr for children and adults and Pb for children. Significantly, the potential negative health impacts of overexposure to Cr include lung and stomach cancer, pneumonia, and renal effects (Dayan & Paine, 2001; Entwistle et al., 2019), while chronic exposure to Pb can cause irreparable renal failure and decrements in intelligence quotients in children (Jose & Srimuruganandam, 2020; Wijayawardena et al., 2016).

Table 10. Exposure assessment and non-carcinogenic and carcinogenic risks for children and adults as a result of exposure to HMs in the road dust of Wadi El-Qamar area.

HMs	Children				Adults			
Exposure assessment								
	Ingestion	**Inhalation**	**Dermal contact**		**Ingestion**	**Inhalation**	**Dermal contact**	
Co	4.72E-05	1.32E-09	1.32E-07		5.06E-06	7.44E-10	2.02E-08	
Cr	9.22E-04	2.59E-08	2.58E-06		9.88E-05	1.45E-08	3.94E-07	
Cu	9.02E-04	2.53E-08	2.52E-06		9.66E-05	1.42E-08	3.85E-07	
Pb	5.36E-04	1.50E-08	1.50E-06		5.75E-05	8.45E-09	2.29E-07	
Zn	2.68E-03	7.53E-08	7.52E-06		2.88E-04	4.23E-08	1.15E-06	
Non-carcinogenic risks								
	HQ_{ing}	**HQ_{inh}**	**HQ_{derm}**	**HI**	**HQ_{ing}**	**HQ_{inh}**	**HQ_{derm}**	**HI**
Co	2.36E-03	2.31E-04	8.25E-06	2.60E-03	2.53E-04	1.30E-04	1.26E-06	3.85E-04
Cr	3.07E-01	9.06E-04	4.30E-02	3.51E-01	3.29E-02	5.07E-04	6.57E-03	4.00E-02
Cu	2.26E-02	6.29E-07	2.10E-04	2.28E-02	2.42E-03	3.53E-07	3.21E-05	2.45E-03
Pb	1.53E-01	4.26E-06	2.86E-03	1.56E-01	1.64E-02	2.40E-06	4.36E-04	1.69E-02
Zn	8.93E-03	2.51E-07	1.25E-04	9.06E-03	9.60E-04	1.41E-07	1.92E-05	9.79E-04
Carcinogenic risks								
	CR_{ing}	**CR_{inh}**	**CR_{derm}**	**TCR**	**CR_{ing}**	**CR_{inh}**	**CR_{derm}**	**TCR**
Cr	4.61E-04	1.29E-08	1.29E-06	4.62E-04	4.94E-05	7.26E-09	1.97E-07	4.96E-05
Pb	4.56E-06	1.28E-10	1.28E-08	4.57E-06	4.88E-07	7.18E-11	1.95E-09	4.90E-07

4. Conclusions

In a preliminary study, the environmental geochemistry of HMs in the road dust of the industrial area of Wadi El-Qamar was studied to evaluate the impact of unplanned industrialization and urbanization. Based on the study findings, the heavy metals were classified into two groups, according to the degree of impact by human activities (1) metals of predominantly natural origin (Fe, Mn, and Co) and (2) metals of dominantly anthropogenic origin (Mo, Cu, Zn, Pb, and Cr). In particular, HMs were not influenced by certain factors as complex input sources have impacted their enrichment; however, Cu, Zn, and Pb were mainly attributed to traffic emissions, while Mo and Cr were suggested to originate from industrial sources. Hence, traffic emissions and industrial activities are the two principal sources of metal-enriched levels in RD samples from the study area. Therefore, to improve public health in Wadi El-Qamar area, governmental actions are needed, including (1) demolishing homes and compensating the residents, with priority given to those whose homes are very adjacent to factories, (2) applying environmental laws to factories and enforcing them to reduce emissions, and (3) setting a road dust management program with a recommendation of regularly watering the road surface to minimize the re-suspension of particles. Furthermore, the environmental situation calls for permanent monitoring of HM levels, sources, and adsorption mechanisms. Besides, future studies should evaluate HM contents in other urban sediments (e.g., roadside soils and beach sediments) in addition to investigating organic contaminants (e.g., polycyclic aromatic hydrocarbons).

Ethics approval and consent to participate: This article does not contain any studies of human participants or animals performed by any of the authors.

Consent for publication: All authors declare their consent for publication.

Funding: The authors declare that no funds, grants, or other support were received during the preparation of this manuscript.

Conflicts of Interest: The author declares no conflict of interest.

Contribution of Authors: Mouataz T. Mostafa: Conceptualization, Writing - original draft. Habash El-Nady: Visualization, Software. Ramadan M. Gomaa: Methodology, Writing - original draft. Salman A. Salman: Investigation, Formal analysis. Ibrahim H. Khalifa: Supervision, Writing - review & editing.

Acknowledgement: The authors acknowledged the laboratory assistance rendered by the Desert Research Center, Cairo, Egypt.

5. References

Abu-Allaban, M., Gillies, J. A., Gertler, A. W., Clayton, R., & Proffitt, D. (2003). Tailpipe, resuspended road dust, and brake-wear emission factors from on-road vehicles. *Atmospheric Environment*, *37*(37), 5283–5293. https://doi.org/10.1016/j.atmosenv.2003.05.005

Adachi, K., & Tainosho, Y. (2004). Characterization of heavy metal particles embedded in tire dust. *Environment International*, *30*(8), 1009–1017. https://doi.org/10.1016/j.envint.2004.04.004

Adamiec, E., Jarosz-Krzemińska, E., & Wieszała, R. (2016). Heavy metals from non-exhaust vehicle emissions in urban and motorway road dusts. *Environmental Monitoring and Assessment*, *188*(6), 369. https://doi.org/10.1007/s10661-016-5377-1

Adimalla, N. (2020). Heavy metals contamination in urban surface soils of Medak province, India, and its risk assessment and spatial distribution. *Environmental Geochemistry and Health*, *42*(1), 59–75. https://doi.org/10.1007/s10653-019-00270-1

Aguilera, A., Bautista, F., Gutiérrez-Ruiz, M., Ceniceros-Gómez, A. E., Cejudo, R., & Goguitchaichvili, A. (2021). Heavy metal pollution of street dust in the largest city of Mexico, sources and health risk assessment. *Environmental Monitoring and Assessment*, *193*(4), 193. https://doi.org/10.1007/s10661-021-08993-4

Ahmed, F., & Ishiga, H. (2006). Trace metal concentrations in street dusts of Dhaka city, Bangladesh. *Atmospheric Environment*, *40*(21), 3835–3844. https://doi.org/10.1016/j.atmosenv.2006.03.004

Al-Khashman, O. A. (2007). The investigation of metal concentrations in street dust samples in Aqaba city, Jordan. *Environmental Geochemistry and Health*, *29*(3), 197–207. https://doi.org/10.1007/s10653-006-9065-x

Alsanad, A., & Alolayan, M. (2020). Heavy metals in road-deposited sediments and pollution indices for different land activities. *Environmental Nanotechnology, Monitoring & Management*, *14*, 100374. https://doi.org/10.1016/j.enmm.2020.100374

Al-Shidi, H. K., Sulaiman, H., Al-Reasi, H. A., Jamil, F., & Aslam, M. (2021). Human and ecological risk assessment of heavy metals in different particle sizes of road dust in Muscat, Oman. *Environmental Science and Pollution Research*, *28*(26), 33980–33993. https://doi.org/10.1007/s11356-020-09319-6

Amato, F., Alastuey, A., de la Rosa, J., Gonzalez Castanedo, Y., Sánchez de la Campa, A. M., Pandolfi, M., Lozano, A., Contreras González, J., & Querol, X. (2014). Trends of road dust emissions contributions on ambient air particulate levels at rural, urban and industrial sites in southern Spain. *Atmospheric Chemistry and Physics*, *14*(7), 3533–3544. https://doi.org/10.5194/acp-14-3533-2014

Amato, F., Querol, X., Johansson, C., Nagl, C., & Alastuey, A. (2010). A review on the effectiveness of street sweeping, washing and dust suppressants as urban PM control methods. *Science of The Total Environment*, *408*(16), 3070–3084. https://doi.org/10.1016/j.scitotenv.2010.04.025

Ameh, E. G., Kolawole, M. S., Idakwo, S. O., Ameh, C. O., & GabrielImeokparia, E. (2016). Distributional Coefficients and Enrichment Studies of Potentially Toxic Heavy Metals in Soils Around Itakpe Iron-Ore Mine, North Central Nigeria. *Earth Science Research*, *6*(1), 85. https://doi.org/10.5539/esr.v6n1p85

Apeagyei, E., Bank, M. S., & Spengler, J. D. (2011). Distribution of heavy metals in road dust along an urban-rural gradient in Massachusetts. *Atmospheric Environment*, *45*(13), 2310–2323. https://doi.org/10.1016/j.atmosenv.2010.11.015

Arslan, H. (2001). HEAVY METALS IN STREET DUST IN BURSA, TURKEY. *Journal of Trace and Microprobe Techniques*, *19*(3), 439–445. https://doi.org/10.1081/TMA-100105058

Baensch-Baltruschat, B., Kocher, B., Stock, F., & Reifferscheid, G. (2020). Tyre and road wear particles (TRWP)—A review of generation, properties, emissions, human health risk, ecotoxicity, and fate in the environment. *Science of The Total Environment*, *733*, 137823. https://doi.org/10.1016/j.scitotenv.2020.137823

Banat, K. M., Howari, F. M., & Al-Hamad, A. A. (2005). Heavy metals in urban soils of central Jordan: Should we worry about their environmental risks? *Environmental Research*, *97*(3), 258–273. https://doi.org/10.1016/j.envres.2004.07.002

Bhuiyan, M. A. H., Parvez, L., Islam, M. A., Dampare, S. B., & Suzuki, S. (2010). Heavy metal pollution of coal mine-affected agricultural soils in the northern part of Bangladesh. *Journal of Hazardous Materials*, *173*(1–3), 384–392. https://doi.org/10.1016/j.jhazmat.2009.08.085

Bourliva, A., Christophoridis, C., Papadopoulou, L., Giouri, K., Papadopoulos, A., Mitsika, E., & Fytianos, K. (2017). Characterization, heavy metal content and health risk assessment of urban road dusts from the historic center of the city of Thessaloniki, Greece. *Environmental Geochemistry and Health*, *39*(3), 611–634. https://doi.org/10.1007/s10653-016-9836-y

Bozlaker, A., Spada, N. J., Fraser, M. P., & Chellam, S. (2014). Elemental Characterization of $PM_{2.5}$ and PM_{10} Emitted from Light Duty Vehicles in the Washburn Tunnel of Houston, Texas: Release of Rhodium, Palladium, And Platinum. *Environmental Science & Technology*, *48*(1), 54–62. https://doi.org/10.1021/es4031003

Buat-Menard, P., & Chesselet, R. (1979). Variable influence of the atmospheric flux on the trace metal chemistry of oceanic suspended matter. *Earth and Planetary Science Letters*, *42*(3), 399–411. https://doi.org/10.1016/0012-821X(79)90049-9

Budai, P., & Clement, A. (2018). Spatial distribution patterns of four traffic-emitted heavy metals in urban road dust and the resuspension of brake-emitted particles: Findings of a field study. *Transportation Research Part D: Transport and Environment*, *62*, 179–185. https://doi.org/10.1016/j.trd.2018.02.014

Cai, Y., Li, F., Zhang, J., Zhu, X., Li, Y., Fu, J., Chen, X., & Liu, C. (2021). Toxic metals in size-fractionated road dust from typical industrial district: Seasonal distribution, bioaccessibility and stochastic-fuzzy health risk management. *Environmental Technology & Innovation*, *23*, 101643. https://doi.org/10.1016/j.eti.2021.101643

Cao, S., Duan, X., Zhao, X., Wang, B., Ma, J., Fan, D., Sun, C., He, B., Wei, F., & Jiang, G. (2015). Health risk assessment of various metal(loid)s via multiple exposure pathways on children living near a typical lead-acid battery plant, China. *Environmental Pollution*, *200*, 16–23. https://doi.org/10.1016/j.envpol.2015.02.010

Cao, Z., Chen, Q., Wang, X., Zhang, Y., Wang, S., Wang, M., Zhao, L., Yan, G., Zhang, X., Zhang, Z., Yang, T., Shen, M., & Sun, J. (2018). Contamination characteristics of trace metals in dust from different levels of roads of a heavily air-polluted city in north China. *Environmental Geochemistry and Health*, *40*(6), 2441–2452. https://doi.org/10.1007/s10653-018-0110-3

Charlesworth, S., De Miguel, E., & Ordóñez, A. (2011). A review of the distribution of particulate trace elements in urban terrestrial environments and its application to considerations of risk. *Environmental Geochemistry and Health*, *33*(2), 103–123. https://doi.org/10.1007/s10653-010-9325-7

Chatterjee, A., & Banerjee, R. N. (1999). Determination of lead and other metals in a residential area of greater Calcutta. *Science of The Total Environment*, *227*(2–3), 175–185. https://doi.org/10.1016/S0048-9697(99)00026-1

Choi, J. Y., Jeong, H., Choi, K.-Y., Hong, G. H., Yang, D. B., Kim, K., & Ra, K. (2020). Source identification and implications of heavy metals in urban roads for the coastal pollution in a beach town, Busan, Korea. *Marine Pollution Bulletin*, *161*, 111724. https://doi.org/10.1016/j.marpolbul.2020.111724

Dall'Osto, M., Thorpe, A., Beddows, D. C. S., Harrison, R. M., Barlow, J. F., Dunbar, T., Williams, P. I., & Coe, H. (2010). *Remarkable dynamics of nanoparticles in the urban atmosphere* [Preprint]. Aerosols/Field Measurements/Troposphere/Physics (physical properties and processes). https://doi.org/10.5194/acpd-10-30651-2010

Dat, N. D., Nguyen, V.-T., Vo, T.-D.-H., Bui, X.-T., Bui, M.-H., Nguyen, L. S. P., Nguyen, X.-C., Tran, A. T.-K., Nguyen, T.-T.-A., Ju, Y.-R., Huynh, T.-M.-T., Nguyen, D.-H., Bui, H.-N., & Lin, C. (2021).

Contamination, source attribution, and potential health risks of heavy metals in street dust of a metropolitan area in Southern Vietnam. *Environmental Science and Pollution Research*, *28*(36), 50405–50419. https://doi.org/10.1007/s11356-021-14246-1

Dayan, A. D., & Paine, A. J. (2001). Mechanisms of chromium toxicity, carcinogenicity and allergenicity: Review of the literature from 1985 to 2000. *Human & Experimental Toxicology*, *20*(9), 439–451. https://doi.org/10.1191/096032701682693062

Denby, B. R., Sundvor, I., Johansson, C., Pirjola, L., Ketzel, M., Norman, M., Kupiainen, K., Gustafsson, M., Blomqvist, G., & Omstedt, G. (2013). A coupled road dust and surface moisture model to predict non-exhaust road traffic induced particle emissions (NORTRIP). Part 1: Road dust loading and suspension modelling. *Atmospheric Environment*, *77*, 283–300. https://doi.org/10.1016/j.atmosenv.2013.04.069

Diami, S. M., Kusin, F. M., & Madzin, Z. (2016). Potential ecological and human health risks of heavy metals in surface soils associated with iron ore mining in Pahang, Malaysia. *Environmental Science and Pollution Research*, *23*(20), 21086–21097. https://doi.org/10.1007/s11356-016-7314-9

Duong, T. T. T., & Lee, B.-K. (2011). Determining contamination level of heavy metals in road dust from busy traffic areas with different characteristics. *Journal of Environmental Management*, *92*(3), 554–562. https://doi.org/10.1016/j.jenvman.2010.09.010

Ebqa'ai, M., & Ibrahim, B. (2017). Application of multivariate statistical analysis in the pollution and health risk of traffic-related heavy metals. *Environmental Geochemistry and Health*, *39*(6), 1441–1456. https://doi.org/10.1007/s10653-017-9930-9.

Ekoa Bessa, A. Z., Ambassa Bela, V., Ngueutchoua, G., El-Amier, Y. A., Aonsi Kamani, F., Ngueudong Zebaze, L., Kamguem Fotso, C. A., Njimanu Njong, V., Kemgang Ghomsi, F. E., Valipour, M., & Armstrong-Altrin, J. S. (2022). Characteristics and Source Identification of Environmental Trace Metals in Beach Sediments Along the Littoral Zone of Cameroon. *Earth Systems and Environment*, *6*(1), 175–187. https://doi.org/10.1007/s41748-021-00279-6.

Ekoa Bessa, A. Z., Ngueutchoua, G., Kwewouo Janpou, A., El-Amier, Y. A., Njike Njome Mbella Nguetnga, O.-A., Kankeu Kayou, U. R., Bisse, S. B., Ngo Mapuna, E. C., & Armstrong-Altrin, J. S. (2021). Heavy metal contamination and its ecological risks in the beach sediments along the Atlantic Ocean (Limbe coastal fringes, Cameroon). *Earth Systems and Environment*, *5*(2), 433–444. https://doi.org/10.1007/s41748-020-00167-5.

El-Geziry, T. M. (2021). Analysis of long-term rainfall and air temperature patterns in Alexandria (Egypt). *Arabian Journal of Geosciences*, *14*(13), 1199. https://doi.org/10.1007/s12517-021-07589-z.

Entwistle, J. A., Hursthouse, A. S., Marinho Reis, P. A., & Stewart, A. G. (2019). Metalliferous Mine Dust: Human Health Impacts and the Potential Determinants of Disease in Mining Communities. *Current Pollution Reports*, *5*(3), 67–83. https://doi.org/10.1007/s40726-019-00108-5.

Fan, P., Lu, X., Yu, B., Fan, X., Wang, L., Lei, K., Yang, Y., Zuo, L., & Rinklebe, J. (2022). Spatial distribution, risk estimation and source apportionment of potentially toxic metal(loid)s in resuspended megacity street dust. *Environment International*, *160*, 107073. https://doi.org/10.1016/j.envint.2021.107073

Fan, X., Lu, X., Yu, B., Zuo, L., Fan, P., Yang, Y., Zhuang, S., Liu, H., & Qin, Q. (2021). Risk and sources of heavy metals and metalloids in dust from university campuses: A case study of Xi'an, China. *Environmental Research*, *202*, 111703. https://doi.org/10.1016/j.envres.2021.111703

Ferreira-Baptista, L., & De Miguel, E. (2005). Geochemistry and risk assessment of street dust in Luanda, Angola: A tropical urban environment. *Atmospheric Environment*, *39*(25), 4501–4512. https://doi.org/10.1016/j.atmosenv.2005.03.026

Gao, D., Ripley, S., Weichenthal, S., & Godri Pollitt, K. J. (2020). Ambient particulate matter oxidative potential: Chemical determinants, associated health effects, and strategies for risk management. *Free Radical Biology and Medicine*, *151*, 7–25. https://doi.org/10.1016/j.freeradbiomed.2020.04.028

Gopal, V., Krishnakumar, S., Simon Peter, T., Nethaji, S., Suresh Kumar, K., Jayaprakash, M., & Magesh, N. S. (2017). Assessment of trace element accumulation in surface sediments off Chennai coast after a major flood event. *Marine Pollution Bulletin*, *114*(2), 1063–1071. https://doi.org/10.1016/j.marpolbul.2016.10.019

Grigoratos, T., & Martini, G. (2015). Brake wear particle emissions: A review. *Environmental Science and Pollution Research*, *22*(4), 2491–2504. https://doi.org/10.1007/s11356-014-3696-8.

Gulia, S., Goyal, P., Goyal, S. K., & Kumar, R. (2019). Re-suspension of road dust: Contribution, assessment and control through dust suppressants—a review. *International Journal of Environmental Science and Technology*, *16*(3), 1717–1728. https://doi.org/10.1007/s13762-018-2001-7.

Guney, M., Onay, T. T., & Copty, N. K. (2010). Impact of overland traffic on heavy metal levels in highway dust and soils of Istanbul, Turkey. *Environmental Monitoring and Assessment*, *164*(1–4), 101–110. https://doi.org/10.1007/s10661-009-0878-9.

Guo, G., Wu, F., Xie, F., & Zhang, R. (2012). Spatial distribution and pollution assessment of heavy metals in urban soils from southwest China. *Journal of Environmental Sciences*, *24*(3), 410–418. https://doi.org/10.1016/S1001-0742(11)60762-6.

Guo, W., Liu, X., Liu, Z., & Li, G. (2010). Pollution and Potential Ecological Risk Evaluation of Heavy Metals in the Sediments around Dongjiang Harbor, Tianjin. *Procedia Environmental Sciences*, *2*, 729–736. https://doi.org/10.1016/j.proenv.2010.10.084.

Hakanson, L. (1980). An ecological risk index for aquatic pollution control.a sedimentological approach. *Water*

Research, *14*(8), 975–1001. https://doi.org/10.1016/0043-1354(80)90143-8.

Han, X., Lu, X., Zhang, Q., Wuyuntana, Hai, Q., & Pan, H. (2016). Grain-size distribution and contamination characteristics of heavy metal in street dust of Baotou, China. *Environmental Earth Sciences*, *75*(6), 468. https://doi.org/10.1007/s12665-016-5316-z.

Harb, M. K., Ebqa'ai, M., Al-rashidi, A., Alaziqi, B. H., Al Rashdi, M. S., & Ibrahim, B. (2015). Investigation of selected heavy metals in street and house dust from Al-Qunfudah, Kingdom of Saudi Arabia. *Environmental Earth Sciences*, *74*(2), 1755–1763. https://doi.org/10.1007/s12665-015-4184-2.

Harrison, R. M., Jones, A. M., Gietl, J., Yin, J., & Green, D. C. (2012). Estimation of the Contributions of Brake Dust, Tire Wear, and Resuspension to Nonexhaust Traffic Particles Derived from Atmospheric Measurements. *Environmental Science & Technology*, *46*(12), 6523–6529. https://doi.org/10.1021/es300894r.

Hong, N., Guan, Y., Yang, B., Zhong, J., Zhu, P., Ok, Y. S., Hou, D., Tsang, D. C. W., Guan, Y., & Liu, A. (2020). Quantitative source tracking of heavy metals contained in urban road deposited sediments. *Journal of Hazardous Materials*, *393*, 122362. https://doi.org/10.1016/j.jhazmat.2020.122362.

Huang, J., Li, F., Zeng, G., Liu, W., Huang, X., Xiao, Z., Wu, H., Gu, Y., Li, X., He, X., & He, Y. (2016). Integrating hierarchical bioavailability and population distribution into potential eco-risk assessment of heavy metals in road dust: A case study in Xiandao District, Changsha city, China. *Science of The Total Environment*, *541*, 969–976. https://doi.org/10.1016/j.scitotenv.2015.09.139.

Huang, Y.-N., Dang, F., Li, M., Zhou, D.-M., Song, Y., & Wang, J.-B. (2020). Environmental and human health risks from metal exposures nearby a Pb-Zn-Ag mine, China. *Science of The Total Environment*, *698*, 134326. https://doi.org/10.1016/j.scitotenv.2019.134326.

Hulskotte, J. H. J., Roskam, G. D., & Denier van der Gon, H. A. C. (2014). Elemental composition of current automotive braking materials and derived air emission factors. *Atmospheric Environment*, *99*, 436–445. https://doi.org/10.1016/j.atmosenv.2014.10.007

Hwang, H.-M., Fiala, M. J., Park, D., & Wade, T. L. (2016). Review of pollutants in urban road dust and stormwater runoff: Part 1. Heavy metals released from vehicles. *International Journal of Urban Sciences*, *20*(3), 334–360. https://doi.org/10.1080/12265934.2016.1193041.

Jadoon, W. A., Abdel-Dayem, S. M. M. A., Saqib, Z., Takeda, K., Sakugawa, H., Hussain, M., Shah, G. M., Rehman, W., & Syed, J. H. (2021). Heavy metals in urban dusts from Alexandria and Kafr El-Sheikh, Egypt: Implications for human health. *Environmental Science and Pollution Research*, *28*(2), 2007–2018. https://doi.org/10.1007/s11356-020-08786-1.

Jaradat, Q. M., Momani, K. A., Jbarah, A.-A. Q., & Massadeh, A. (2004). Inorganic analysis of dust fall and office dust in an industrial area of Jordan. *Environmental Research*, *96*(2), 139–144. https://doi.org/10.1016/j.envres.2003.12.005.

Jiménez, M. D., de Torre, R., Mola, I., Casado, M. A., & Balaguer, L. (2018). Local plant responses to global problems: Dactylis glomerata responses to different traffic pollutants on roadsides. *Journal of Environmental Management*, *212*, 440–449. https://doi.org/10.1016/j.jenvman.2017.12.049.

Jose, J., & Srimuruganandam, B. (2020). Investigation of road dust characteristics and its associated health risks from an urban environment. *Environmental Geochemistry and Health*, *42*(9), 2819–2840. https://doi.org/10.1007/s10653-020-00521-6.

Kabata-Pendias, A., & Pendias, H. (2001). *Trace elements in soils and plants* (3rd ed). CRC Press.

Kabir, Md. H., Kormoker, T., Islam, Md. S., Khan, R., Shammi, R. S., Tusher, T. R., Proshad, R., Islam, M. S., & Idris, A. M. (2021). Potentially toxic elements in street dust from an urban city of a developing country: Ecological and probabilistic health risks assessment. *Environmental Science and Pollution Research*, *28*(40), 57126–57148. https://doi.org/10.1007/s11356-021-14581-3.

Kamani, H., Mirzaei, N., Ghaderpoori, M., Bazrafshan, E., Rezaei, S., & Mahvi, A. H. (2018). Concentration and ecological risk of heavy metal in street dusts of Eslamshahr, Iran. *Human and Ecological Risk Assessment: An International Journal*, *24*(4), 961–970. https://doi.org/10.1080/10807039.2017.1403282

Karim, Z., Qureshi, B. A., Mumtaz, M., & Qureshi, S. (2014). Heavy metal content in urban soils as an indicator of anthropogenic and natural influences on landscape of Karachi—A multivariate spatio-temporal analysis. *Ecological Indicators*, *42*, 20–31. https://doi.org/10.1016/j.ecolind.2013.07.020.

Kelepertzis, E. (2014). Investigating the sources and potential health risks of environmental contaminants in the soils and drinking waters from the rural clusters in Thiva area (Greece). *Ecotoxicology and Environmental Safety*, *100*, 258–265. https://doi.org/10.1016/j.ecoenv.2013.09.030.

Kelly, F. J., & Fussell, J. C. (2012). Size, source and chemical composition as determinants of toxicity attributable to ambient particulate matter. *Atmospheric Environment*, *60*, 504–526. https://doi.org/10.1016/j.atmosenv.2012.06.039.

Khan, M. N., Wasim, A. A., Sarwar, A., & Rasheed, M. F. (2011). Assessment of heavy metal toxicants in the roadside soil along the N-5, National Highway, Pakistan. *Environmental Monitoring and Assessment*, *182*(1–4), 587–595. https://doi.org/10.1007/s10661-011-1899-8.

Li, F., Zhang, J., Huang, J., Huang, D., Yang, J., Song, Y., & Zeng, G. (2016). Heavy metals in road dust from Xiandao District, Changsha City, China: Characteristics, health risk assessment, and integrated source identification. *Environmental Science and Pollution Research*, *23*(13), 13100–13113. https://doi.org/10.1007/s11356-016-6458-y.

Liu, A., Hong, N., Zhu, P., & Guan, Y. (2019). Characterizing petroleum hydrocarbons deposited on road surfaces in urban environments. *Science of The Total Environment*, *653*, 589–596. https://doi.org/10.1016/j.scitotenv.2018.10.428.

Liu, B., Wang, J., Xu, M., Zhao, L., & Wang, Z. (2019). Spatial distribution, source apportionment and ecological risk assessment of heavy metals in the sediments of Haizhou Bay national ocean park, China. *Marine Pollution Bulletin*, *149*, 110651. https://doi.org/10.1016/j.marpolbul.2019.110651.

Liu, M., Yang, Y., Yun, X., Zhang, M., & Wang, J. (2015). Concentrations, distribution, sources, and ecological risk assessment of heavy metals in agricultural topsoil of the Three Gorges Dam region, China. *Environmental Monitoring and Assessment*, *187*(3), 147. https://doi.org/10.1007/s10661-015-4360-6.

Logiewa, A., Miazgowicz, A., Krennhuber, K., & Lanzerstorfer, C. (2020). Variation in the Concentration of Metals in Road Dust Size Fractions Between 2 µm and 2 mm: Results from Three Metallurgical Centres in Poland. *Archives of Environmental Contamination and Toxicology*, *78*(1), 46–59. https://doi.org/10.1007/s00244-019-00686-x

Maanan, M., Saddik, M., Maanan, M., Chaibi, M., Assobhei, O., & Zourarah, B. (2015). Environmental and ecological risk assessment of heavy metals in sediments of Nador lagoon, Morocco. *Ecological Indicators*, *48*, 616–626. https://doi.org/10.1016/j.ecolind.2014.09.034.

Malakootian, M., Mohammadi, A., Nasiri, A., Asadi, A. M. S., Conti, G. O., & Faraji, M. (2021). Spatial distribution and correlations among elements in smaller than 75 µm street dust: Ecological and probabilistic health risk assessment. *Environmental Geochemistry and Health*, *43*(1), 567–583. https://doi.org/10.1007/s10653-020-00694-0.

Mandal, A., & Voutchkov, M. (2011). Heavy Metals in Soils around the Cement Factory inRockfort, Kingston, Jamaica. *International Journal of Geosciences*, *02*(01), 48–54. https://doi.org/10.4236/ijg.2011.21005.

Miguel, E. de, Llamas, J. F., Chacón, E., Berg, T., Larssen, S., Røyset, O., & Vadset, M. (1997). Origin and patterns of distribution of trace elements in street dust: Unleaded petrol and urban lead. *Atmospheric Environment*, *31*(17), 2733–2740. https://doi.org/10.1016/S1352-2310(97)00101-5.

Mostafa, M. T., Nady, H. El., Gomaa, R. M., Abdelgawad, H. F., Farhat, H. I., Khalifa, I. H., & Salman, S. A. (2023). Geochemical Baseline and Pre-Mining Environmental Assessment of Heavy Metals at Iron Exploration Area, Northeastern Aswan, Egypt. *Water, Air, & Soil Pollution*, *234*(7), 456. https://doi.org/10.1007/s11270-023-06466-7

Muller, G. (1969). Index of geoaccumulation in sediments of the Rhine River. *Geojournal*, *2*, 108–118.

Najmeddin, A., Keshavarzi, B., Moore, F., & Lahijanzadeh, A. (2018). Source apportionment and health risk assessment of potentially toxic elements in road dust from urban industrial areas of Ahvaz megacity, Iran. *Environmental Geochemistry and Health*, *40*(4), 1187–1208. https://doi.org/10.1007/s10653-017-0035-2.

Nazzal, Y., Ghrefat, H., & Rosen, M. A. (2013). Application of multivariate geostatistics in the investigation of heavy metal contamination of roadside dusts from selected highways of the Greater Toronto Area, Canada. *Environmental Earth Sciences*, *71*(3), 1409–1419. https://doi.org/10.1007/s12665-013-2546-1.

Okbah, M. A., Ibrahim, A. M. A., & Gamal, M. N. M. (2013). Environmental monitoring of linear alkylbenzene sulfonates and physicochemical characteristics of seawater in El-Mex Bay (Alexandria, Egypt). *Environmental Monitoring and Assessment*, *185*(4), 3103–3115. https://doi.org/10.1007/s10661-012-2776-9.

Pan, H., Lu, X., & Lei, K. (2017). A comprehensive analysis of heavy metals in urban road dust of Xi'an, China: Contamination, source apportionment and spatial distribution. *Science of The Total Environment*, *609*, 1361–1369. https://doi.org/10.1016/j.scitotenv.2017.08.004.

Pang, H.-J., Lou, Z.-H., Jin, A.-M., Yan, K.-K., Jiang, Y., Yang, X.-H., Arthur Chen, C.-T., & Chen, X.-G. (2015). Contamination, distribution, and sources of heavy metals in the sediments of Andong tidal flat, Hangzhou bay, China. *Continental Shelf Research*, *110*, 72–84. https://doi.org/10.1016/j.csr.2015.10.002

Pellinen, V., Cherkashina, T., & Gustaytis, M. (2021). Assessment of metal pollution and subsequent ecological risk in the coastal zone of the Olkhon Island, Lake Baikal, Russia. *Science of The Total Environment*, *786*, 147441. https://doi.org/10.1016/j.scitotenv.2021.147441

Polukarova, M., Markiewicz, A., Björklund, K., Strömvall, A.-M., Galfi, H., Andersson Sköld, Y., Gustafsson, M., Järlskog, I., & Aronsson, M. (2020). Organic pollutants, nano- and microparticles in street sweeping road dust and washwater. *Environment International*, *135*, 105337. https://doi.org/10.1016/j.envint.2019.105337.

Rahman, M. S., Kumar, P., Ullah, M., Jolly, Y. N., Akhter, S., Kabir, J., Begum, B. A., & Salam, A. (2021). Elemental analysis in surface soil and dust of roadside academic institutions in Dhaka city, Bangladesh and their impact on human health. *Environmental Chemistry and Ecotoxicology*, *3*, 197–208. https://doi.org/10.1016/j.enceco.2021.06.001

Saeedi, M., Li, L. Y., & Salmanzadeh, M. (2012). Heavy metals and polycyclic aromatic hydrocarbons: Pollution and ecological risk assessment in street dust of Tehran. *Journal of Hazardous Materials*, *227–228*, 9–17. https://doi.org/10.1016/j.jhazmat.2012.04.047

Safiur Rahman, M., Khan, M. D. H., Jolly, Y. N., Kabir, J., Akter, S., & Salam, A. (2019). Assessing risk to human health for heavy metal contamination through street dust in the Southeast Asian Megacity: Dhaka, Bangladesh. *Science of The Total Environment*, *660*, 1610–1622. https://doi.org/10.1016/j.scitotenv.2018.12.425.

Said, I., Hursthouse, A., & Salman, S. A. E.-R. (2021). Identification of pollution sources in roadside soils of Cairo-Alexandria Highway, Egypt. *Arabian Journal of Geosciences*, *14*(11), 981. https://doi.org/10.1007/s12517-021-07360-4.

Shahab, A., Zhang, H., Ullah, H., Rashid, A., Rad, S., Li, J., & Xiao, H. (2020). Pollution characteristics and toxicity of potentially toxic elements in road dust of a tourist city, Guilin, China: Ecological and health risk assessment☆. *Environmental Pollution*, *266*, 115419. https://doi.org/10.1016/j.envpol.2020.115419.

Shimod, K. P., Vineethkumar, V., Prasad, T. K., & Jayapal, G. (2022). Effect of urbanization on heavy metal contamination: A study on major townships of Kannur District in Kerala, India. *Bulletin of the National Research Centre*, *46*(1), 4. https://doi.org/10.1186/s42269-021-00691-y.

Shreadah, M. A., Shobier, A. H., Ghani, S. A. A., El Zokm, G. M., & Said, T. O. (2015). Major ions anomalies and contamination status by trace metals in sediments from two hot spots along the Mediterranean Coast of Egypt. *Environmental Monitoring and Assessment*, *187*(5), 280. https://doi.org/10.1007/s10661-015-4420-y.

Smedley, P. L., Cooper, D. M., Ander, E. L., Milne, C. J., & Lapworth, D. J. (2014). Occurrence of molybdenum in British surface water and groundwater: Distributions, controls and implications for water supply. *Applied Geochemistry*, *40*, 144–154. https://doi.org/10.1016/j.apgeochem.2013.03.014.

Smedley, P. L., & Kinniburgh, D. G. (2017). Molybdenum in natural waters: A review of occurrence, distributions and controls. *Applied Geochemistry*, *84*, 387–432. https://doi.org/10.1016/j.apgeochem.2017.05.008.

Sultan, M. B., Choudhury, T. R., Alam, Md. N.-E., Doza, Md. B., & Rahmana, Md. M. (2022). Soil, dust, and leaf-based novel multi-sample approach for urban heavy metal contamination appraisals in a megacity, Dhaka, Bangladesh. *Environmental Advances*, *7*, 100154. https://doi.org/10.1016/j.envadv.2021.100154.

Tan, Z., Lu, S., Zhao, H., Kai, X., Jiaxian, P., Win, M. S., Yu, S., Yonemochi, S., & Wang, Q. (2018). Magnetic, geochemical characterization and health risk assessment of road dust in Xuanwei and Fuyuan, China. *Environmental Geochemistry and Health*, *40*(4), 1541–1555. https://doi.org/10.1007/s10653-018-0070-7.

Tomlinson, D. L., Wilson, J. G., Harris, C. R., & Jeffrey, D. W. (1980). Problems in the assessment of heavy-metal levels in estuaries and the formation of a pollution index. *Helgoländer Meeresuntersuchungen*, *33*(1–4), 566–575. https://doi.org/10.1007/BF02414780.

Tong, R., Fang, Y., Zhang, B., Wang, Y., & Yang, X. (2021). Monitoring and evaluating the control effect of dust suppressant on heavy metals based on ecological and health risks: A case study of Beijing. *Environmental Science and Pollution Research*, *28*(12), 14750–14763. https://doi.org/10.1007/s11356-020-11648-5.

Trojanowska, M., & Świetlik, R. (2019). Investigations of the chemical distribution of heavy metals in street dust and its impact on risk assessment for human health, case study of Radom (Poland). *Human and Ecological Risk Assessment: An International Journal*, *26*(7), 1907–1926. https://doi.org/10.1080/10807039.2019.1619070.

Trujillo-González, J. M., Torres-Mora, M. A., Keesstra, S., Brevik, E. C., & Jiménez-Ballesta, R. (2016). Heavy metal accumulation related to population density in road dust samples taken from urban sites under different land uses. *Science of The Total Environment*, *553*, 636–642. https://doi.org/10.1016/j.scitotenv.2016.02.101.

Turekian, K. K., & Wedepohl, K. H. (1961). Distribution of the Elements in Some Major Units of the Earth's Crust. *Geological Society of America Bulletin*, *72*(2), 175. https://doi.org/10.1130/0016-7606(1961)72[175:DOTEIS]2.0.CO;2.

USEPA. (1989). *Risk Assessment Guidance for Superfund*. U.S. Environmental Protection Agency, Office of Emergency and Remedial Response.

USEPA. (1996a). *Method 3050B acid digestion of sediments, sludges, and soils 1.0 scope and application*. US Environmental Protection Agency.

USEPA. (1996b). *Soil Screening Guidance: User's Guide*. U.S. Environmental Protection Agency: Office of Emergency and Remedial Response.

USEPA. (2002a). *Child-Specific Exposure Factors Handbook*. U.S. Environmental Protection Agency, National Center for Environmental Assessment, Office of Research and Development.

USEPA. (2002b). *SUPPLEMENTAL GUIDANCE FOR DEVELOPING SOIL SCREENING LEVELS FOR SUPERFUND SITES*. U.S. Environmental Protection Agency: Office of Emergency and Remedial Response.

USEPA. (2004). *Risk Assessment Guidance for Superfund. Volume I: Human Health Evaluation Manual-part E, supplemental guidance for dermal risk assessment*. U.S. Environmental Protection Agency: Office of superfund remediation and technology innovation.

USEPA. (2005). *Guidelines for Carcinogen Risk Assessment*. U.S. Environmental Protection Agency, Risk Assessment Forum.

USEPA. (2011). *Exposure Factors Handbook*. U.S. Environmental Protection Agency.

USEPA. (2012). *EPA's Integrated Risk Information System Program*. U.S. Environmental Protection Agency: Office of Research and Development.

Vanegas, S., Trejos, E. M., Aristizábal, B. H., Pereira, G. M., Hernández, J. M., Murillo, J. H., Ramírez, O., Amato, F., Silva, L. F. O., Rojas, N. Y., Zafra, C., & Pachón, J. E. (2021). Spatial Distribution and Chemical Composition of Road Dust in Two High-Altitude Latin American Cities. *Atmosphere*, *12*(9), 1109. https://doi.org/10.3390/atmos12091109.

Varol, M. (2011). Assessment of heavy metal contamination in sediments of the Tigris River (Turkey) using pollution indices and multivariate statistical techniques. *Journal of Hazardous Materials*, *195*, 355–364. https://doi.org/10.1016/j.jhazmat.2011.08.051.

Wang, W., Qin, Y., Song, D., & Wang, K. (2008). Column leaching of coal and its combustion residues, Shizuishan, China. *International Journal of Coal Geology*, *75*(2), 81–87. https://doi.org/10.1016/j.coal.2008.02.004.

Wang, X., Liu, E., Lin, Q., Liu, L., Yuan, H., & Li, Z. (2020). Occurrence, sources and health risks of toxic metal(loid)s in road dust from a mega city (Nanjing) in China. *Environmental Pollution*, *263*, 114518. https://doi.org/10.1016/j.envpol.2020.114518.

Wedepohl, K. H. (1995). The composition of the continental crust. *Geochimicaet Cosmochimica Acta*, *59*(7), 1217–1232.

Wijayawardena, M. A. A., Megharaj, M., & Naidu, R. (2016). Exposure, Toxicity, Health Impacts, and Bioavailability of Heavy Metal Mixtures. In *Advances in Agronomy* (Vol. 138, pp. 175–234). Elsevier. https://doi.org/10.1016/bs.agron.2016.03.002.

Wiseman, C. L. S., Levesque, C., & Rasmussen, P. E. (2021). Characterizing the sources, concentrations and resuspension potential of metals and metalloids in the thoracic fraction of urban road dust. *Science of The Total Environment*, *786*, 147467. https://doi.org/10.1016/j.scitotenv.2021.147467.

Wu, S., Peng, S., Zhang, X., Wu, D., Luo, W., Zhang, T., Zhou, S., Yang, G., Wan, H., & Wu, L. (2015). Levels and health risk assessments of heavy metals in urban soils in Dongguan, China. *Journal of Geochemical Exploration*, *148*, 71–78. https://doi.org/10.1016/j.gexplo.2014.08.009.

Xu, S., Zheng, N., Liu, J., Wang, Y., & Chang, S. (2013). Geochemistry and health risk assessment of arsenic exposure to street dust in the zinc smelting district, Northeast China. *Environmental Geochemistry and Health*, *35*(1), 89–99. https://doi.org/10.1007/s10653-012-9463-1.

Yang, T., Liu, Q., Li, H., Zeng, Q., & Chan, L. (2010). Anthropogenic magnetic particles and heavy metals in the road dust: Magnetic identification and its implications. *Atmospheric Environment*, *44*(9), 1175–1185. https://doi.org/10.1016/j.atmosenv.2009.12.028

Yesilkanat, C. M., & Kobya, Y. (2021). Spatial characteristics of ecological and health risks of toxic heavy metal pollution from road dust in the Black Sea coast of Turkey. *Geoderma Regional*, *25*, e00388. https://doi.org/10.1016/j.geodrs.2021.e00388.

Yuen, J. Q., Olin, P. H., Lim, H. S., Benner, S. G., Sutherland, R. A., & Ziegler, A. D. (2012). Accumulation of potentially toxic elements in road deposited sediments in residential and light industrial neighborhoods of Singapore. *Journal of Environmental Management*, *101*, 151–163. https://doi.org/10.1016/j.jenvman.2011.11.017.

Zafra, C., Temprano, J., & Suárez, J. (2017). A simplified method for determining potential heavy metal loads washed-off by stormwater runoff from road-deposited sediments. *Science of The Total Environment*, *601–602*, 260–270. https://doi.org/10.1016/j.scitotenv.2017.05.178.

Zgłobicki, W., Telecka, M., & Skupiński, S. (2019). Assessment of short-term changes in street dust pollution with heavy metals in Lublin (E Poland)—Levels, sources and risks. *Environmental Science and Pollution Research*, *26*(34), 35049–35060. https://doi.org/10.1007/s11356-019-06496-x.

Zgłobicki, W., Telecka, M., Skupiński, S., Pasierbińska, A., & Kozieł, M. (2018). Assessment of heavy metal contamination levels of street dust in the city of Lublin, E Poland. *Environmental Earth Sciences*, *77*(23), 774. https://doi.org/10.1007/s12665-018-7969-2.

Zhang, J., Wu, J., Hua, P., Zhao, Z., Wu, L., Fan, G., Bai, Y., Kaeseberg, T., & Krebs, P. (2017). The influence of land use on source apportionment and risk assessment of polycyclic aromatic hydrocarbons in road-deposited sediment. *Environmental Pollution*, *229*, 705–714. https://doi.org/10.1016/j.envpol.2017.07.019.

Zhao, N., Lu, X., Chao, S., & Xu, X. (2015). Multivariate statistical analysis of heavy metals in less than 100 μm particles of street dust from Xining, China. *Environmental Earth Sciences*, *73*(5), 2319–2327. https://doi.org/10.1007/s12665-014-3578-x.

Zheng, N., Liu, J., Wang, Q., & Liang, Z. (2010). Heavy metals exposure of children from stairway and sidewalk dust in the smelting district, northeast of China. *Atmospheric Environment*, *44*(27), 3239–3245. https://doi.org/10.1016/j.atmosenv.2010.06.002

Zhong, C., Yang, Z., Jiang, W., Hu, B., Hou, Q., Yu, T., & Li, J. (2016). Ecological geochemical assessment and source identification of trace elements in atmospheric deposition of an emerging industrial area: Beibu Gulf economic zone. *Science of The Total Environment*, *573*, 1519–1526. https://doi.org/10.1016/j.scitotenv.2016.08.057.

Žibret, G. (2019). Influences of coal mines, metallurgical plants, urbanization and lithology on the elemental composition of street dust. *Environmental Geochemistry and Health*, *41*(3), 1489–1505. https://doi.org/10.1007/s10653-018-0228-3.

تحديد المصدر وحالة التلوث وتقييم المخاطر البيئية للتلوث بالعناصر الثقيلة في منطقة صناعية غير مخططة ذات كثافة سكانية عالية (وادي القمر)، الإسكندرية، مصر

معتز طارق مصطفى[١]، وحبش النادي[١]، ورمضان محمد جمعة[١]، وسلمان عبد الرؤف سلمان[٢]، وإبراهيم حسين خليفة[٣]

[١]قسم الجيولوجيا، كلية العلوم، جامعة العريش، شمال سيناء، مصر

[٢]قسم العلوم الجيولوجية، المركز القومي للبحوث، الجيزة، مصر

[٣]قسم الجيولوجيا، كلية العلوم، جامعة قناة السويس، الإسماعيلية، مصر

تم إجراء دراسة للجيوكيمياء البيئية لغبار الطرق بمنطقة وادي القمر بمحافظة الإسكندرية التي تعد منطقة صناعية وسكانية غير مخططة، وذلك لتقييم تأثير النشاط الصناعي والبشري بها. فجاء ترتيب متوسطات تركيز العناصر على النحو التالي: الحديد> المنجنيز> الزنك> الكروميوم> النحاس> الرصاص> الموليبدنوم> الكوبلت. وصنفت العناصر الثقيلة محل الدراسة حسب درجة تأثير الأنشطة البشرية في معدل تراكمها إلى مجموعتين: (١) عناصر من أصل طبيعي في المقام الأول (الحديد والمنجنيز والكوبلت)؛ (٢) عناصر من أصل بشري (النحاس والرصاص والكروميوم والزنك والموليبدنوم)، حيث تم ربط وجود النحاس والزنك والرصاص بشكل رئيسي إلى انبعاثات عوادم السيارات واحتكاك الإطارات مع سطح الطريق، ولا سيما المركبات الثقيلة. كما اقترح ارتباط الموليبدنوم والكروميوم بمصادر صناعية خاصةً مصانع الأسمنت وشركات تكرير الزيوت. لذلك، لتحسين الصحة العامة في منطقة وادي القمر، هناك حاجة لاتخاذ إجراءات حكومية بهدم المنازل ونقل السكان وتعويضهم، مع إعطاء الأولوية لمن تكون منازلهم قريبة جدًا من المصانع، وكذا تشجيع المصانع على تسريع وتيرة التحول للعمل باستخدام الطاقة النظيفة.